Journal of Physiology (2002), **541.3**, *pp.* 779–796
DOI: 10.1113/jphysiol.2002.018887

www.jphysiol.org

Rho family GTP binding proteins are involved in the regulatory volume decrease process in NIH3T3 mouse fibroblasts

Stine F. Pedersen *, Kristine H. Beisner *, Charlotte Hougaard *, Berthe M. Willumsen †, Ian H. Lambert * and Else K. Hoffmann *

* *Department of Biochemistry, August Krogh Institute and † Department of Molecular Cell Biology, University of Copenhagen, Denmark*

The role of Rho GTPases in the regulatory volume decrease (RVD) process following osmotic cell swelling is controversial and has so far only been investigated for the swelling-activated Cl^- efflux. We investigated the involvement of RhoA in the RVD process in NIH3T3 mouse fibroblasts, using wild-type cells and three clones expressing constitutively active RhoA (RhoAV14). RhoAV14 expression resulted in an up to fourfold increase in the rate of RVD, measured by large-angle light scattering. The increase in RVD rate correlated with RhoAV14 expression. RVD in wild-type cells was unaffected by the Rho kinase inhibitor Y-27632 and the phosphatidyl-inositol 3 kinase (PI3K) inhibitor wortmannin. The maximal rates of swelling-activated K^+ ($^{86}Rb^+$ as tracer) and taurine ([^{3}H]taurine as tracer) efflux after a 30 % reduction in extracellular osmolarity were increased about twofold in cells with maximal RhoAV14 expression compared to wild-type cells, but were unaffected by Y-27632. The volume set points for activation of release of both osmolytes appeared to be reduced by RhoAV14 expression. The maximal taurine efflux rate constant was potentiated by the tyrosine phosphatase inhibitor Na_3VO_4, and inhibited by the tyrosine kinase inhibitor genistein. The magnitude of the swelling-activated Cl^- current ($I_{Cl,swell}$) was higher in RhoAV14 than in wild-type cells after a 7.5 % reduction in extracellular osmolarity, but, in contrast to $^{86}Rb^+$ and [^{3}H]taurine efflux, similar in both strains after a 30 % reduction in extracellular osmolarity. $I_{Cl,swell}$ was inhibited by Y-27632 and strongly potentiated by the myosin light chain kinase inhibitors ML-7 and AV25. It is suggested that RhoA, although not the volume sensor *per se*, is an important upstream modulator shared by multiple swelling-activated channels on which RhoA exerts its effects via divergent signalling pathways.

(Received 14 February 2002; accepted after revision 27 March 2002)
Corresponding author E. K. Hoffmann: August Krogh Institute,13, Universitetsparken, Dk-2100 Copenhagen, Denmark. Email: ekhoffmann@aki.ku.dk

In essentially all mammalian cells, osmotic cell swelling triggers a chain of events leading to net loss of Cl^-, K^+, organic osmolytes such as taurine, and osmotically obliged water, and resulting in cell volume recovery, a process known as regulatory volume decrease (RVD) (see e.g. Hoffmann & Dunham, 1995). The early events activated by swelling of mammalian cells and resulting in activation of osmolyte release pathways are still far from understood. Several lines of evidence suggest that the actin-based cytoskeleton may play a role in the initial sensing and/or subsequent transduction of the signal of volume change (for reviews see e.g. Henson, 1999; Hoffmann & Mills, 1999; Pedersen *et al.* 2001*a*). Membrane unfolding and concomitant changes in cortical F-actin organisation have been suggested to modulate the volume sensitivity of $I_{Cl,swell}$ (Okada, 1997), and there is also evidence indicating that swelling-activated efflux of taurine (Ding *et al.* 1998) and K^+ (Cantiello *et al.* 1993) is modulated by cytoskeletal components. Swelling-induced F-actin reorganisation, most commonly involving a depolymerisation of cortical F-actin, has been demonstrated in several cell types (e.g. Hallows *et al.* 1991; Pedersen *et al.* 1999; see Pedersen *et al.* 2001*a*), including NIH3T3 cells (Pedersen *et al.* 2001*b*). The mechanisms involved in eliciting osmotically induced F-actin changes are poorly understood, but swelling-induced stress-fibre formation in bovine aortic endothelial cells was recently found to involve small GTP binding (G) proteins of the Rho family, indicating that these proteins may be activated by cell swelling (Koyama *et al.* 2001).

The Rho family G proteins, including Cdc42, Rac (isoforms 1, 2 and 3), and Rho (isoforms A, B and C), play pivotal roles in F-actin organisation (see e.g. Bishop & Hall, 2000) and integrin signalling (see Schwartz & Shattil, 2000). Their activity is regulated by interaction with guanine nucleotide exchange factors (GEFs) and guanine nucleotide dissociation inhibitors (GDIs), which respectively stimulate

and inhibit exchange of GTP for GDP on the G proteins, and by GTPase activating proteins (GAPs), which stimulate their intrinsic GTPase activity (see e.g. Takai *et al.* 2001). Upstream from these regulators, the Rho GTPases are activated in response to e.g. mitogens, lysophosphatidic acid, integrin activation, and various biological stressors (Bishop & Hall, 2000; Schwartz & Shattil, 2000). An important downstream effector of Rho is the Rho-associated kinase (p164ROKα and p160ROKβ/ROCK). One consequence of ROK/ROCK activitation is increased myosin light chain (MLC) phosphorylation, to which ROK/ROCK contributes both directly, and indirectly via inhibition of MLC phosphatase (see e.g. Somlyo & Somlyo, 2000). The latter appears to be the relevant mechanism *in vivo*, implying that substantial MLC phosphorylation cannot be induced by ROK/ROCK activity alone, but also requires the activity of MLC kinase (MLCK) and/or another MLC-phosphorylating kinase (ibid.). Other Rho effectors include phosphatidylinositol 4-phosphate 5-kinase (PI4P5 kinase), mDia and phosphatidylinositol 3-kinase (PI3K), the latter possibly acting via the focal adhesion kinase (FAK), all of which are thought to contribute to Rho-mediated F-actin reorganisation (see e.g. Tilly *et al.* 1996; Bishop & Hall, 2000; Takai *et al.* 2001).

GTPγS has been shown to stimulate, and GDPβS to inhibit, RVD (Margalit *et al.* 1993; Thoroed *et al.* 1997; Shen *et al.* 1998) as well as $I_{Cl,swell}$ (e.g. Voets *et al.* 1998; Estevez *et al.* 2001), suggesting a role for G proteins in the process. In some cases, this appears to at least partly reflect the involvement of heterotrimeric G protein-coupled receptors (GPCRs; Lambert, 1989; Shen *et al.* 1998; Shimizu *et al.* 2000; see Hoffmann & Hougaard, 2001), or other processes coupled to heterotrimeric G proteins, such as activation of a $cPLA_2$ (Margalit *et al.* 1993; Thoroed *et al.* 1997). Three groups have proposed the involvement of small G proteins of the Rho family in the swelling-induced activation of $I_{Cl,swell}$, all via different pathways. In Intestine 407 cells, Rho was reported to activate FAK, leading to activation of PI3K and subsequently $I_{Cl,swell}$ (Tilly *et al.* 1996). In calf pulmonary artery endothelial (CPAE) cells, Rho-induced activation of $I_{Cl,swell}$ was proposed to be mediated via ROK/ROCK, possibly in part via increased MLC phosphorylation (Nilius *et al.* 1999; Nilius *et al.* 2000). Finally, in mouse neuroblastoma cells, both a Rho family G protein and a cholera toxin-sensitive, heterotrimeric G protein were suggested to be involved in the activation of $I_{Cl,swell}$, apparently in a phosphorylation-independent manner (Estevez *et al.* 2001).

In many cell types, tyrosine kinases are activated by cell swelling and are involved in the RVD process (see e.g. Lang *et al.* 1998). Tyrosine kinases are generally found to stimulate, and tyrosine phosphatases to inhibit, the swelling-activated efflux of Cl^- (e.g. Voets *et al.* 1998) as well as of taurine (Deleuze *et al.* 2000; Lambert & Falktoft, 2000). Whereas some findings suggest a link between the activation of small G proteins and tyrosine kinases in the activation of volume regulatory transporters after osmotic cell swelling (Tilly *et al.* 1996), others do not lend support to this notion (Deleuze *et al.* 2000).

Thus, the signalling events linking Rho to activation of $I_{Cl,swell}$ remain incompletely understood, and other possible roles of Rho in the RVD process than the above-mentioned effects on $I_{Cl,swell}$ have, to the best of our knowledge, not been directly addressed. Similar to many other cell types, NIH3T3 mouse fibroblasts are known to exhibit RVD through the activation of efflux pathways for K^+, Cl^- and organic osmolytes such as taurine (Pasantes-Morales *et al.* 1997; Moran *et al.* 1997). In this study, we compare the swelling-induced activation of Cl^-, K^+ and taurine efflux in wild-type NIH3T3 cells and NIH3T3 cells expressing constitutively active RhoA, in order to evaluate the roles of RhoA and Rho effectors in the RVD process in an integrated manner.

Part of this study has previously been presented in abstract form (Pedersen *et al.* 2001*b*).

METHODS

Chemicals

Unless otherwise stated, chemicals were purchased from Sigma Aldrich (St Louis, MO, USA) or Mallinckrodt Baker B.V. (Deventer, Netherlands).

Monoclonal antibodies to the Myc epitope tag (9E10; sc-40) and to Rho/ROCK (sc-1852) were obtained from Santa Cruz Biotechnology, Santa Cruz, CA, USA (sc-40), and horseradish peroxidase (HRP)-conjugated secondary antibody (rabbit anti-mouse IgG) from Dako, Denmark. Chemiluminescence ECL (enhanced chemiluminescence) was from Amersham Life Science, Buckinghamshire, UK. Y27632 was a kind gift from Welfide Corporation (Osaka, Japan), and was dissolved (5 mM) in H_2O. The MLCK inhibitory peptide AV25 (AKKLAKDRMKKY-MARRKLQKAGHAV) (Weber *et al.* 1999), was a kind gift from Professor M. P. Walsh, University of Calgary, Canada, and was dissolved at 0.1 mM in 10 mM TRIS-HCl, pH 7.5. ML-7 (Calbiochem, Darmstadt, Germany) was dissolved at 5 mM in 50 % ethanol. All these reagents were stored at 5 °C until use. On the day of the experiment, clotrimazole was dissolved (10 mM) in dry DMSO, tetraethylammonium chloride (TEA, 1 M), $BaCl_2$ (0.5 M) and clofilium tosylate (RBI, Natick, MA, USA; 5 mM) in H_2O, and furosemide (0.5 M) in methanol. [^{3}H]Taurine and $^{86}Rb^+$ were obtained from Amersham. $GdCl_3$ was dissolved (60 mM) in H_2O and stored at room temperature until use. Charybdotoxin (ChTX, Alomone Labs, Jerusalem, Israel) was dissolved in experimental medium enriched with 0.1 % BSA (25 μM), agitoxin-2 (1 μM) and Na_3VO_4 (20 mM) (Alomone Labs) in H_2O, niflumic acid and 4,4′-diisothiocyano-2,2′-stilbene-disulfonic acid (DIDS) (both 100 mM) in DMSO, and tamoxifen (10 mM) in methanol. All these reagents were stored at −20 °C until use. Fura 2-AM and rhodamine-conjugated phalloidin (Molecular Probes, Leiden, Netherlands) were dissolved at 10 mM in dry DMSO and 200 U ml^{-1} in methanol, respectively, and stored at −20 °C until use.

Cell culture, transfection and immunoblotting

The NIH3T3 fibroblasts (clone 7) were obtained from Douglas Lowy, NIH, Bethesda, MD, USA. Stable cell lines expressing activating mutations of RhoA (RhoAV14, pEXVmyctagV14 Rho; Ridley & Hall, 1992), Rac1 (Rac1V12, pEXVmyctagV12Rac; Ridley *et al.* 1992), both from Alan Hall, MRC, UK, and H-Ras (G12R and A59T, pBW 1423; Willumsen *et al.* 1991) were selected from pools of plasmid-transfected cells as described previously (Willumsen, 1995).

RhoAV14 and Rac1V12 clones were chosen after Western blot analysis of the myc-tagged protein. Cell lysates were prepared by washing twice in phosphate buffered saline (PBS), and scraping off the cells (using a 'rubber policeman') in 2 × SDS sample buffer (0.06 M Tris-HCl, pH 6.8, 5 % SDS, 25 % glycerol, 0.075 % bromphenol blue, 0.7 M β-mercaptoethanol) supplemented with 200 mM DTT. The extract was sheared with a 27G needle and boiled for 5 min. Equal amounts of lysate (30 μl in each lane) were separated by 12.5 % SDS-PAGE, and transferred to polyvinylidene difluoride (PVDF) membranes. The membranes were blocked (PBS, 2 % Tween-20, 5 % dry milk) for 45 min, incubated at 4 °C overnight with monoclonal anti-myc antibody (1:1000 in PBS, 0.075 % Tween-20, 5 % dry milk), followed by HRP-conjugated secondary antibody (1:5000 in PBS, 0.075 % Tween-20, 5 % dry milk) for 1 h at room temp, followed by visualisation by ECL chemiluminescence. An estimation of band intensity led to the selection of three clones with different levels of RhoAV14 expression. Cross reaction to an endogenous protein or blotting for an endogenous protein showed similar protein concentrations in the extract.

Cells were cultured in Dulbecco's modified Eagle's medium supplemented with 10 % fetal calf serum and 10 ml l^{-1} penicillin–streptomycin, at 37 °C, 5 % CO_2, 95 % humidity. Cultures were passaged every 3–4 days. Only passages 10–30 were used. Unless otherwise indicated, experiments were performed at 37 °C.

Estimation of changes in cell volume and free, intracellular calcium concentration ($[Ca^{2+}]_i$)

Light scatter and $[Ca^{2+}]_i$ measurements. Estimation of relative cell volume was performed using large-angle light scattering, essentially as described by McManus *et al.* (1993). Cells were seeded 24 h prior to experiments on rectangular (10 mm × 50 mm), HCl- and ethanol-washed coverslips (confluency at the time of experiments 70–80 %). For experiments, the coverslips were placed at a 50 deg angle relative to the excitation light in the cuvette of a PTI RatioMaster spectrophotometer with a 75 W xenon lamp. The excitation wavelength was 577 nm, and emission was measured at 580 nm. The standard isotonic NaCl medium contained (mM): 150 NaCl, 1 Na_2HPO_4, 1 $CaCl_2$, 10 Hepes, 5 glucose, pH 7.4. In hypotonic medium, osmolarity was reduced by 50 % by removal of NaCl. The cells were continuously perfused at 0.7 ml min^{-1} with the experimental medium, and rapid solution changes were induced by briefly increasing flow to maximum level (3.5 ml min^{-1}). Data are given as the inverse of the 580 nm emission, as emitted light intensity correlates inversely with cell volume. RVD and RVI rates were calculated as the slope of the relative cell volume traces within the initial 90 s following maximal cell swelling or shrinkage, respectively.

In some experiments, changes in the free intracellular calcium concentration ($[Ca^{2+}]_i$) were assessed simultaneously with the cell volume measurements, by preloading the cells with 2 μM fura-2-AM in the standard isotonic medium for 20 min at 37 °C prior to experiments and measuring at 510 nm after excitation at 340 and 380 nm. Data were evaluated as the 340 nm/380 nm ratio. Fura-2 loading did not affect the light scatter measurements.

Coulter counter measurements. Cells grown to about 80–90 % confluency in 150 cm^2 culture flasks were detached by brief treatment with a Ca^{2+}- and Mg^{2+}-free trypsin/EGTA solution, followed by gentle centrifugation (30 s, 700 *g*), and resuspension in isotonic NaCl solution (composition as for efflux experiments, see below). After 20 min incubation with gentle shaking at 37 °C, experiments were initiated by diluting the cells in filtered (0.45 μm filters, Milipore) isotonic NaCl solution. Distribution curves were obtained using electronic cell sizing (Coulter Multisizer II, 100 μm tube orifice). Absolute cell volumes were calculated from the median of the distribution curves after calibration with latex beads (19.6 μm diameter, Coulter Electronics, Luton, UK).

Electrophysiology

NIH3T3 fibroblasts were seeded thinly on 25 mm glass coverslips 24–48 h prior to whole-cell patch-clamp experiments. The coverslips were mounted on a temperature-controlled chamber installed on an inverted microscope (Zeiss Axiovert 10, Carl Zeiss, Germany). Whole-cell recordings were performed while the cells were superfused at 1.5–2.0 ml min^{-1} with the experimental solution in a 500 μl volume chamber. Bath and pipette solutions were chosen to enable Cl^- current measurements. The composition of the 30 % hypotonic bath solution was (mM): 125 NaCl, 2.5 $CaCl_2$, 2.5 $MgCl_2$, 10 Hepes, pH 7.2 (adjusted with NaOH). Bath solutions of 15 % and 7.5 % hypotonicity were prepared by appropriate mixing of isotonic and 30 % hypotonic solutions. The isotonic bath solution was made from the hypotonic solution by addition of 75 mM D-mannitol. The pipette solution was (mM): 150 $CsCl_2$, 5 $MgCl_2$, 10 Hepes, 10 EGTA, 2 ATP, 0.1 GTP, pH 7.2 (adjusted with CsOH). The measured osmolarities were about 330, 300, 290, 250, and 340 mosmol l^{-1} for the isotonic, 7.5 %, 15 %, 30 % hypotonic, and internal (pipette) solutions, respectively. The pipettes were made from Vitrex glass capillary tubing with an outside diameter of 1.7 mm (Modulohm, Herlev, Denmark) using a Narishige PP-830 puller (Tokyo, Japan) and had resistances of 4 MΩ.

After obtaining a gigaohm seal between the pipette and the cell membrane, the patch was ruptured by applying gentle suction. Currents were measured in the whole-cell configuration of the patch-clamp technique using an Axopatch 200B (Axon Instruments, Union City, CA, USA) amplifier and all current measurements were filtered at 2 kHz. A Digidata 1200 Interface board and pCLAMP7 software (Axon Instruments) were used to generate voltage-clamp command voltages and to digitise data. The holding potential was −40 mV. The following voltage protocol was used in most experiments, and was applied every 10 s: a 500 ms step to −60 mV, a 200 ms step to −80 mV, followed by a 2.6 s linear voltage ramp to +80 mV. A step protocol was also applied in some experiments: from the holding potential of −40 mV, 20 mV steps of 1000 ms duration were applied from −80 to +80 mV. The whole-cell capacitance was read from the compensation dials of the patch-clamp amplifier and used as an estimate of cell surface area, and hence, cell size. Corrections for junction potential were calculated using pCLAMP software. Percentage inhibition of the current by Cl^- channel inhibitors was calculated from the difference in stable current magnitude before and after perfusion with the inhibitor, after full activation of the current.

[^{3}H]Taurine and $^{86}Rb^+$ efflux measurements

The [^{3}H]taurine and $^{86}Rb^+$ efflux measurements were performed simultaneously, at room temperature, essentially as previously described (Lambert & Falktoft, 2000). Cells were grown to 80 % confluency in 35 mm diameter polyethylene dishes and loaded with [^{3}H]taurine (2135 Bq ml^{-1}) and $^{86}Rb^+$ (40 000 Bq ml^{-1}) for 2 h at 37 °C. At the end of the loading period, the cells were washed four times in isotonic experimental solution to remove extracellular isotope. The standard isotonic efflux medium contained (mM): 150 NaCl, 1 Na_2HPO_4, 1 $CaCl_2$, 10 Hepes, pH 7.4 (adjusted with NaOH). In hypotonic medium, osmolarity was reduced by 33 or 50 % by removal of NaCl. The efflux experiments were performed by removal/addition of 1 ml aliquots of experimental solution at 2 min intervals. The aliquots removed were transferred to scintillation vials for estimation of [$^3H^+$] and $^{86}Rb^+$ activity (Ultima Gold). At the end of the efflux experiment, the cells were lysed (0.5 M NaOH, 2 h), and the lysate plus two washes (distilled H_2O) were transferred to scintillation vials for estimation of the $^3H^+$ and $^{86}Rb^+$ activity. The total measure of radioactivity was calculated as the sum of radioactivity in all samples plus the activity remaining in the cells at the end of the experiment (lysate plus washes). Data were plotted as the natural logarithm of the fraction of activity remaining in the cells, as a function of time. Efflux rate constants were calculated for each time point as the negative slope of the curve between the time point and the previous time point. From these data, the minimal decrease in extracellular osmolarity needed to produce an efflux significantly larger than the efflux under isotonic conditions was determined using Student's *t* test. It may be noted that the tracer flux experiments were performed at room temperature, while all other experiments were performed at 37 °C. Two flux experiments performed at 37 °C showed, however, firstly, that the increase in swelling-activated $^{86}Rb^+$ and [^{3}H]taurine efflux rates in RhoAV14C3 cells compared to those in wild-type cells observed at room temperature (see Results) was also observed at 37 °C, and secondly, that the isotonic $^{86}Rb^+$ efflux at 37 °C in both strains was almost doubled compared to that measured at room temperature, and thus of a magnitude similar to that measured after cell swelling at 37 °C ($n = 2$, data not shown).

Measurements of cellular F-actin content

Total cellular F-actin content was measured using a quantitative rhodamine–phalloidin binding assay, essentially as described in Pedersen *et al.* (1999). Briefly, cells were seeded 48 h prior to experiments in 12-well polyethylene dishes, and were about 70 % confluent at the time of the experiment. After 1 min exposure to isotonic or 50 % hypotonic medium (with or without 30 min preincubation with 10 μM ML-7) the cells were fixed in paraformaldehyde at a final concentration of 2 % first for 15 min at room temperature, then for 30 min on ice, washed in TBS (150 mM NaCl, 10 mM Tris-HCl, 1 mM $MgCl_2$, 1 mM EGTA, pH 7.4), and permeabilised for 10 min in 0.1 % saponin in Mops buffer (10 mM Mops, 5 mM EGTA, 20 mM K_2HPO_4, 2 mM $MgSO_4$, pH 6.9). Aliqots of cells were incubated with a saturating concentration of rhodamine-phallodin (33 μM) in MOPS buffer with 0.1 % saponin for 1 h, washed in Mops buffer, and incubated with 3 ml of gradient-grade methanol per well for 30 min. The methanol was transferred to a cuvette, and rhodamine fluorescence was measured at 576 nm after excitation at 540 nm, using a PTI Ratiomaster spectrophotometer. The linearity of the assay in the relevant range was verified, and actin-binding specificity was demonstrated by competition of rhodamine fluorescence with a 100-fold excess of unlabelled phalloidin, essentially as described in Pedersen *et al.* (1999). Data are presented as the 576 nm emission after subtraction of a methanol blank, and are given relative to the corresponding isotonic control.

Statistical analysis

Data are shown as means ± standard error of the mean (S.E.M.) or as individual experiments representative of a minimum of three independent experiments. Student's *t* test (two-sided, unpaired) was used to evaluate statistical significance. *P* values of < 0.05 are taken to indicate a significant difference.

RESULTS

Effect of RhoAV14 expression on the RVD rate in NIH3T3 fibroblasts

In order to study the role of RhoA in the RVD process in NIH3T3 cells, three clones (RhoAV14B1, RhoAV14B4, and RhoAV14C3, in order of increasing RhoAV14 expression) expressing a constitutively active RhoA mutant (RhoAV14) were selected by Western blot analysis of myc-tagged RhoAV14 (Fig. 1*A*). In agreement with the well-established effects of RhoA activity on F-actin organisation (see e.g. Bishop & Hall, 2000), RhoAV14 expression resulted in a substantial increase in stress-fibre formation, and concomitant changes in cell morphology (S. F. Pedersen & E. K. Hoffmann, unpublished observations). Steady state cell volume, measured by electronic cell sizing of detached cells, was increased by about 25 % (2238 ± 113 fl in wild-type cells and 2850 ± 33 fl in RhoAV14C3 cells, $n = 3$ for each clone), and the capacitance, corresponding to plasma membrane area, was increased by about 30 % (24 ± 1.4 pF ($n = 22$) in wild-type cells and 32 ± 3.7 pF ($n = 10$) in RhoAV14C3 cells). Although not further studied here, this long-term difference in cell volume seems likely to reflect the involvement of Rho family G proteins in the control of cell growth and proliferation (Aznar & Lacal, 2001).

Cell volume recovery following swelling in hypotonic solution (50 % reduction of osmolarity compared to isotonic conditions) was subsequently monitored in wild-type cells and in the three RhoAV14 clones using large angle light scattering. Figure 1*B* (wild-type) and *C* (RhoAV14C3) illustrates the time course of cell volume regulation. The rates of RVD, calculated from the volume traces, are shown in Fig. 1*D*. As can be seen, the RVD rate correlated with the level of RhoAV14 expression, reaching a rate of $33 \times 10^{-3} \pm 3.2 \times 10^{-3}$ min^{-1} ($n = 14$) in clone RhoAV14C3, compared to $8 \times 10^{-3} \pm 1.4 \times 10^{-3}$ min^{-1} ($n = 15$) in wild-type cells, i.e. a fourfold increase. The RVD rate was significantly increased in all RhoAV14-expressing strains compared to that of wild-type cells ($P < 0.0001$ for wild-type *vs.* RhoAV14B4 and RhoAV14C3 and < 0.05 for wild-type *vs.* RhoAV13B1, $n = 8$–15). That this is not simply a peculiarity of the high level expression of RhoAV14 is indicated by the fact that the RVD rate in the RhoAV14C3 cells was significantly higher than in the two cell lines with the intermediate (RhoAV14B4, $P < 0.05$) and lowest (RhoAV14B1, $P < 0.0005$) RhoA expression, and that the

rate in RhoAV14B4 cells was significantly higher than in RhoAV14B1 cells ($P < 0.05$).

As can be seen, both wild-type and RhoAV14-expressing strains exhibited volume recovery after osmotic cell swelling. However, in contrast to the wild-type cells, the volume of RhoAV14C3 cells was rapidly regulated back to the isotonic value, and even exhibited an initial 'overshoot' of volume regulation, resulting in a cell volume (in arbitrary units) of 0.95 ± 0.008 ($n = 14$) at time 600 s after hypotonic exposure (see below). Most probably as a result of the very rapid onset of RVD in the RhoAV14C3 cells, the maximal cell swelling measured immediately after hypotonic challenge was decreased by RhoAV14 expression ($n = 15$ wild-type, $n = 14$ RhoAV14C3, data not shown). It

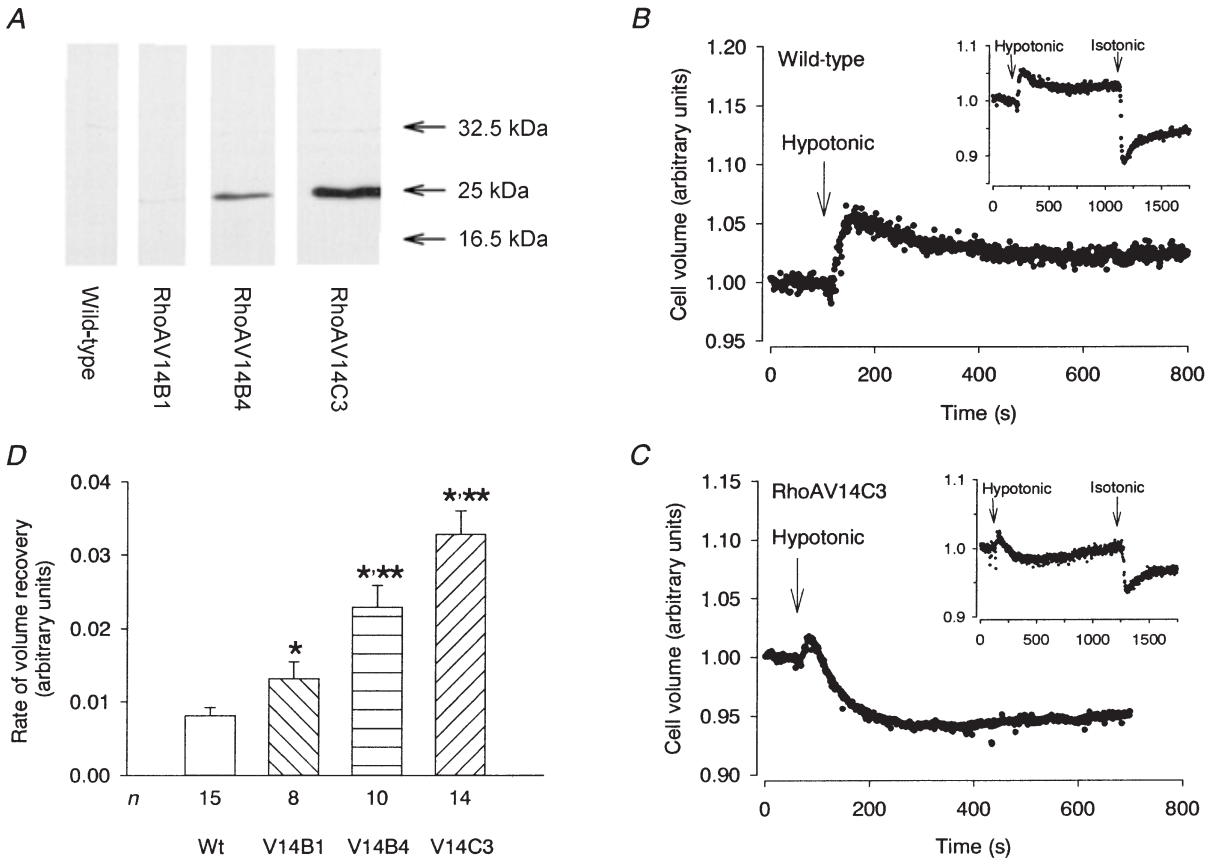

Figure 1. Effect of RhoAV14 expression on the RVD rate after hypotonic cell swelling

A, Western blot analysis of myc-tagged RhoAV14 in wild-type and three RhoAV14 expressing clones of NIH3T3 cells. Cell lysates were subjected to 12.5 % SDS-PAGE, followed by transfer to PVDF membranes. Immunoblotting was performed with a monoclonal antibody against the myc tag on the RhoAV14 protein (seen as an ~25 kDa band), followed by HRP-conjugated secondary antibody and visualisation using ECL. *B*, cell volume changes in wild-type NIH3T3 cells as a function of time after hypotonic exposure. Relative cell volume was monitored in adherent NIH3T3 cells using large angle light scattering, as described in Methods. A hypotonic challenge was induced at the time indicated by the arrow, by rapidly changing the isotonic perfusion solution to a 50 % hypotonic solution. The experiment shown is representative of 15 independent experiments. The insert shows the cell volume changes in the wild-type NIH3T3 cells as a function of time when the cells were allowed to equilibrate in hypotonic medium, and subsequently re-exposed to isotonic medium. The experiment shown is representative of 13 independent experiments. See text for details. *C*, cell volume changes in RhoAV14C3 cells as a function of time after hypotonic exposure. Experimental procedures were as described for *B*. The experiments shown in the main panel and in the inset are representative of 14 independent experiments. *D*, RVD rates in wild-type NIH3T3 cells and three RhoAV14-expressing clones. RVD rates were calculated from light scatter experiments, as shown in *B* and *C*, as the slope of the relative cell volume traces in the initial 90 s after hypotonic exposure. Data are shown as means with S.E.M. error bars, with the number of experiments indicated below each column. The RVD rates were significantly different from those of wild-type cells in all RhoAV14-expressing clones. * Significant difference from the rate in wild-type cells. *P* values were < 0.05 for RhoAV14B1, and < 0.0001 for RhoAV14B4 and RhoAV14C3. ** Significant difference from the rate in RhoAV14B1 cells. *P* values were < 0.0005 for RhoAV14C3 and < 0.05 for RhoAV14B4. The rate in RhoAV14B4 cells was also significantly different from that in RhoAV14C3 cells ($P < 0.05$).

should be noted that the actual increase in cell volume at maximal cell swelling cannot be evaluated from the arbitrary values shown in Fig. 1. Attempts to further investigate this possible difference in osmotic swelling by inhibiting the volume recovery process with channel blockers were unsuccessful due to lack of effective inhibitors of the K^+ efflux pathway (see below). It may be noted, however, that all other things being equal, less osmotic cell swelling should result in a correspondingly smaller RVD rate, i.e. the fourfold increase in RVD rate in RhoAV14-expressing cells relative to that in wild-type cells would be even more striking if the extent of osmotic swelling was actually reduced in RhoAV14C3 cells. Upon cytochalasin treatment (cytochalasin B 10 μM, 10 min), wild-type and RhoAV14C3 cells swell to a similar extent (volume in arbitrary units 1.09 ± 0.016, $n = 4$ for wild-type, and 1.12 ± 0.016, $n = 3$ for RhoAV14C3 cells). Whether this reflects a role for the actin cytoskeleton in the regulation of the volume-activated transporters or in the resistance to swelling is currently under investigation.

As seen in the inset in Fig. 1*C*, after the initial shrinkage below the initial isotonic volume, the volume of the RhoAV14C3 cells gradually recovers towards the steady state volume. To investigate whether the initial 'overshoot' of volume regulation might involve an impairment of the regulatory volume increase (RVI) process in the RhoAV14C3 cells, the cells were re-exposed to isotonic medium after 15–20 min of hypotonicity. After equilibration in hypotonic medium, the isotonic medium is hypertonic with respect to the cell interior. As seen in the inserts in Fig. 1*B* (wild-type cells) and Fig. 1*C* (RhoAV14C3 cells), both cell types responded to this treatment with rapid osmotic shrinkage and subsequent RVI. The initial rate of RVI was 0.020 ± 0.0027 min^{-1} ($n = 13$) in wild-type cells, and 0.030 ± 0.0037 min^{-1} ($n = 14$) in RhoAV14C3 cells, slightly but significantly higher than that in wild-type cells ($P < 0.05$). Thus, the RVI process was intact in the RhoAV14C3 cells. Taken together, this suggests that the most probable cause of the initial shrinkage below isotonic volume in the RhoAV14C3 cells is a slightly prolonged opening of the swelling-activated K^+ and Cl^- channels, and that the resulting 'overshoot' is not large enough to trigger the RVI process (see also Discussion).

Effects of Rac1V12 or H-Ras expression on RVD

To establish whether the stimulatory effect on the RVD rate was specific for RhoA, or might also be evoked by other types of small G proteins, RVD was also monitored in NIH3T3 cells expressing constitutively active Rac1 (Rac1V12) or H-Ras, respectively. In cells expressing Rac1V12, the RVD rate was increased to $18 \times 10^{-3} \pm 4.4 \times 10^{-3}$ min^{-1} ($n = 6$), compared to the $8 \times 10^{-3} \pm 1.4 \times 10^{-3}$ min^{-1} ($n = 15$) calculated in wild-type cells ($P < 0.005$). In contrast, in cells expressing H-Ras, the RVD rate was $5.9 \times 10^{-3} \pm 1.29 \times 10^{-3}$ min^{-1} ($n = 7$), not significantly different from that of wild-type cells.

Possible signal transduction mechanisms involved in the RhoA-mediated acceleration of RVD

In some cell types, osmotic swelling elicits an increase in the free, intracellular calcium concentration, $[Ca^{2+}]_i$, which contributes to activation of the RVD process (see e.g. Hoffmann & Mills, 1999). Therefore, we performed simultaneous measurements of relative cell volume and $[Ca^{2+}]_i$ in order to evaluate whether RhoAV14 expression altered the effect of hypotonic challenge on $[Ca^{2+}]_i$ in the NIH3T3 cells. However, no increases in $[Ca^{2+}]_i$ were detectable upon cell swelling, either in wild-type ($n = 5$) or in RhoAV14-expressing cells ($n = 3$), arguing against a role for global changes in $[Ca^{2+}]_i$ in the RhoA-mediated acceleration of RVD.

As noted above, both ROK/ROCK and PI3K have been suggested to be involved in Rho-mediated events following cell swelling. In wild-type cells, pre-incubation with the ROK/ROCK inhibitor Y-27632 (Uehata *et al.* 1997; Ishizaki *et al.* 2000) (10 μM, 10 min), and with the PI3K inhibitor wortmannin (1 μM, 30 min) resulted in RVD rates of $10 \times 10^{-3} \pm 1.7 \times 10^{-3}$ min^{-1} ($n = 5$), or $7 \times 10^{-3} \pm 3.9 \times 10^{-3}$ min^{-1} ($n = 3$), respectively, compared to $8 \times 10^{-3} \pm 1.4 \times 10^{-3}$ min^{-1} ($n = 15$) in control cells. Thus, neither of these compounds appeared to affect the RVD rate in wild-type NIH3T3 cells.

Effects of RhoA on the swelling-activated osmolyte efflux pathways

As an accelerated RVD response reflects an increased rate of osmolyte release, we subsequently compared the activity of the swelling-activated transport systems in wild-type and RhoAV14-expressing NIH3T3 cells.

Role of RhoA in the swelling-activated K^+ efflux. The K^+ efflux (measured as $^{86}Rb^+$ efflux) was increased within the first few minutes after a 33 % decrease in osmolarity, and the maximal rate of K^+ efflux was obtained about 6 min after the hypotonic challenge in both wild-type and RhoAV14C3 cells (the clone with maximal RhoAV14 expression, and the one used in all subsequent experiments) (Fig. 2*A*). After this time, the rate constant decreased, reflecting the gradual recovery of cell volume. The maximal rate constant for $^{86}Rb^+$ efflux after a 33 % decrease in osmolarity was increased about twofold in RhoAV14C3 cells, to 0.018 ± 0.0012 min^{-1} ($n = 3$), compared to 0.010 ± 0.0016 min^{-1} ($n = 4$) in wild-type cells ($P < 0.005$). Multiplication of the rate constants for the $^{86}Rb^+$ efflux in the wild-type cells by the ratio between the maximal rate constants in wild-type and RhoA cells resulted in an efflux curve that was essentially superimposed on the efflux curves for RhoAV14C3 cells in the time range from 0 to 6 min following hypotonic exposure. This indicates that

the activation kinetics for the swelling-activated $^{86}Rb^+$ efflux were unaffected by RhoAV14 expression. In order to elicit a swelling-activated $^{86}Rb^+$ efflux significantly different from that seen under isotonic conditions, extracellular osmolarity had to be decreased by 33 % in wild-type cells, but by only 22 % in RhoAV14C3 cells (Fig. 2*B*). This suggests that the volume set point for activation of $^{86}Rb^+$ efflux may be reduced by RhoAV14 expression. It is emphasised that absolute volume set points were not determined in the present study, but that the change in set point induced by RhoAV14 expression was evaluated by comparison of the minimal decrease in osmolarity needed to activate an efflux significantly different from the efflux under isotonic conditions in wild-type and RhoAV14-expressing cells. In congruence with this, $^{86}Rb^+$ efflux in RhoAV14C3 cells was significantly different from that measured in wild-type cells when the decrease in extracellular osmolarity was 26 % or greater (Fig. 2*B*). In contrast to the taurine and Cl^- efflux pathways, the swelling-activated K^+ efflux pathway in NIH3T3 cells has, to our knowledge, so far not been pharmacologically characterised. Furosemide (0.5 mM), an inhibitor of the swelling-activated K–Cl cotransporter, and the classical K^+ channel blockers tetraethylammonium (TEA, 10 mM) and Ba^{2+} (2 mM), inhibited the swelling-activated $^{86}Rb^+$ efflux by 38 ± 3.6 %, 32 ± 4.4 % and 21 ± 4.8 %, respectively ($n = 3$). Other K^+ channel blockers tested (gadolinium, 100 μM; agitoxin-2, 5 nM; clofilium, 100 μM; clotrimazole, 1 μM; and charybdotoxin, 100 nM) had little or no effect on the swelling-activated $^{86}Rb^+$ efflux ($n = 3$ for each compound, data not shown). Finally, in wild-type cells, preincubation with the ROK/ROCK inhibitor Y-27632 (10 μM, 10 min) only inhibited the swelling-activated $^{86}Rb^+$ efflux by 10 ± 7.7 % ($n = 3$), arguing against an important role for ROK/ROCK in the activation pathway.

Role of RhoA in the swelling-activated taurine efflux. As seen in Fig. 3*A*, the rate of taurine efflux (monitored as [^{3}H]taurine efflux) after a 33 % decrease in osmolarity was maximal about 6 min after hypotonic challenge in both wild-type and RhoAV14C3 cells. After this time the rate constant decreased, reflecting mainly the recovery of cell volume, and in agreement with previous reports (Moran *et al.* 1997). Similar to the findings for $^{86}Rb^+$ efflux, the maximal rate constant for the swelling-induced taurine efflux was almost twofold higher in RhoAV14C3 cells than in wild-type cells (0.105 ± 0.007 min^{-1}, $n = 3$ in RhoAV14C3 cells, compared to 0.056 ± 0.014 min^{-1}, $n = 4$ in wild-type cells; $P < 0.05$). A comparable potentiation of the swelling-induced taurine efflux was seen after a 50 % decrease in osmolarity, where the maximal rate constants were 0.212 ± 0.0016 and 0.150 ± 0.016 in RhoAV14C3 and wild-type cells, respectively ($n = 4$ for RhoAV14C3 cells and $n = 3$ for wild-type cells, $P < 0.03$). As for the $^{86}Rb^+$ efflux, multiplying the rate constants for the taurine efflux in the wild-type cells by the ratio between the maximal

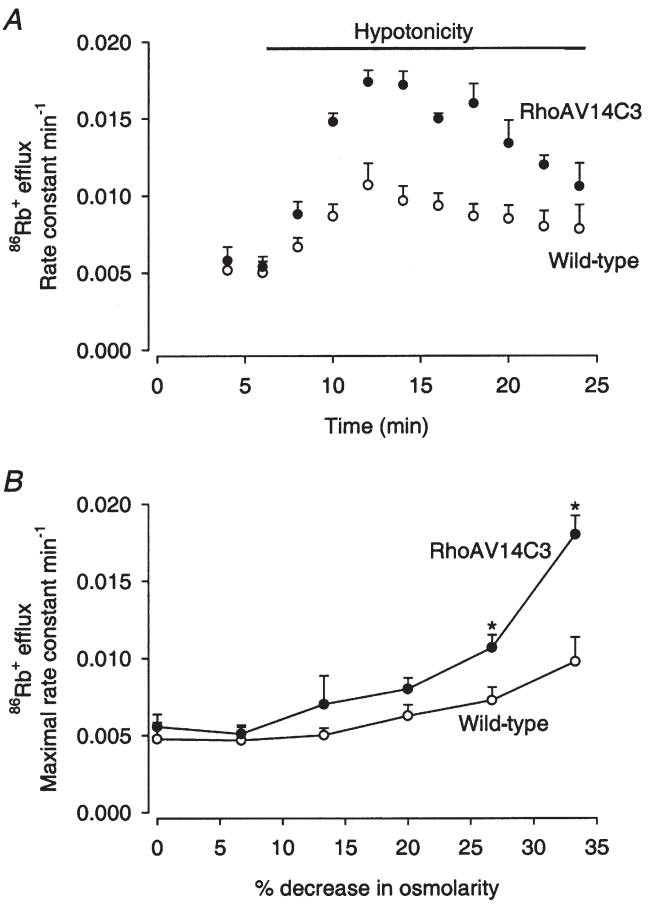

Figure 2. Swelling-activated $^{86}Rb^+$ efflux from NIH3T3 cells

A, effect of RhoAV14 expression on swelling-activated K^+ efflux. Wild-type and RhoAV14C3 cells were preloaded with $^{86}Rb^+$ for 2 h, followed by efflux measurements as described in Methods. At time 6 min, the extracellular osmolarity was reduced by 33 %, from 300 to 200 mosmol l^{-1}. The efflux rate constants shown were obtained from a plot of the natural logarithm of the activity fraction remaining in the cells as a function of time, as the negative slope of the curve between the time point shown and the preceding time point. Rates are shown as means + S.E.M. of 4 (wild-type) or 3 (RhoAV14C3) experiments. *B*, dependence of $^{86}Rb^+$ efflux on osmolarity in wild-type and RhoAV14C3 cells. The $^{86}Rb^+$ efflux was measured as above. At time 6 min, the extracellular osmolarity was reduced by the percentage shown. The figure shows the maximal efflux rate constant, obtained at time 6 min after hypotonic exposure, as a function of the decrease in extracellular osmolarity. Rates are shown as means + S.E.M. of 4 (wild-type) or 3 (RhoAV14C3) experiments. * The value in RhoAV14VC3 cells is significantly different from that in wild-type cells. Swelling-activated $^{86}Rb^+$ efflux is significantly different from that seen under isotonic conditions at a decrease in extracellular osmolarity of 33 % in wild-type cells ($P < 0.05$), and of 22 % or more in RhoAV14C3 cells ($P < 0.05$).

rate constants in wild-type and RhoA cells resulted in essentially superimposed efflux curves, indicating that the activation kinetics for taurine efflux are not altered by RhoA over-expression. Swelling-activated taurine efflux was significantly different from the isotonic value after a decrease in osmolarity of 22 % in the wild-type cells, and 13.3 % in RhoAV14C3 cells (Fig. 3*B*), thus RhoAV14 expression may also slightly reduce the volume set point for this osmolyte. Correspondingly, the swelling-activated taurine efflux in RhoAV14C3 cells was significantly different from that measured in wild-type cells at all decreases in extracellular osmolarity of 20 % or more (Fig. 3*B*). Preincubation with Y-27632 (10 μM, 10 min) had no effect on the swelling-activated taurine efflux in either wild-type or RhoAV14C3 cells, after either 22 % or 33 % decreases in extracellular osmolarity (percentage inhibition 7 ± 6.7 % and 2 ± 2.4 % in wild-type cells, and 6 ± 3.2 % and 2 ± 3.4 % in RhoAV14C3 cells at 22 % and 33 % decreases in osmolarity, respectively, $n = 3$). In wild-type cells, we also found that preincubation with Y-27632 (10 μM, 10 min) had no effect on the maximal rate constant for taurine efflux after a decrease in osmolarity of 50 %, the mean inhibition measured being 2 ± 2.0 % ($n = 3$). Thus, similar to the findings for the overall RVD rate and for $^{86}Rb^+$ efflux, ROK/ROCK does not appear to be involved in the swelling-induced activation of taurine efflux. Finally, preincubation with wortmannin (0.5 μM, 10 min) to inhibit PI3K had no effect on the swelling-activated taurine efflux elicited by a 33 % decrease in osmolarity ($n = 2$, data not shown).

Role of RhoA in the swelling-activated Cl^- efflux. The swelling-activated Cl^- current ($I_{Cl,swell}$) was studied using whole-cell patch-clamp recording, in wild-type and in RhoAV14C3 cells. The pipette solution was buffered at less than 10 nM free calcium using EGTA, and the osmolarity of the bath solution was altered by changing the mannitol content at unaltered ionic strength. In both wild-type and RhoAV14C3 cells, a 30 % decrease in bath osmolarity elicited rapid cell swelling (not shown) and, after a lag time of about 1 min, development of an outwardly rectifying current, which reversed upon re-exposure to isotonic conditions (Fig. 4*A* and *D*). The current could be repetitively activated by multiple hypotonic exposures. The current reversal potential was 0.7 ± 0.26 mV in wild-type cells ($n = 38$) and 0.5 ± 0.33 mV in RhoAV14C3 cells ($n = 30$), in good agreement with the calculated equilibrium potential for a Cl^- current under the present experimental conditions (−0.3 mV). Thus, under these conditions, the current seems to be mainly carried by Cl^-. In both strains, the current exhibited time-dependent inactivation at depolarised potentials (Fig. 4*B* and *E*), and was moderately outward rectifying (Fig. 4*C* and *F*).

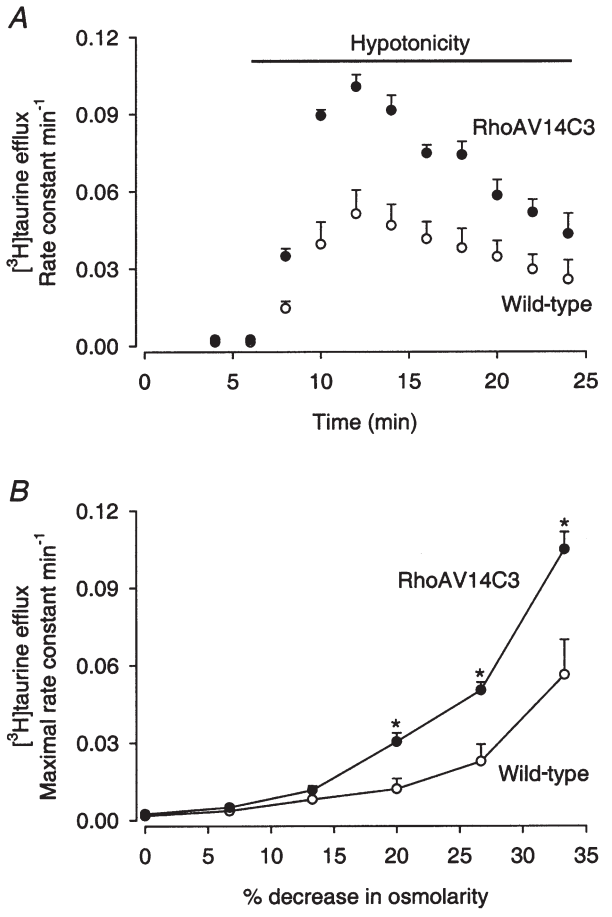

Figure 3. Swelling-activated taurine efflux from NIH3T3 cells

A, effect of RhoAV14 expression on swelling-induced taurine efflux. Wild-type and RhoAV14C3 cells (80 % confluent) were preloaded with [^{3}H]taurine for 2 h, followed by efflux measurements as described in Methods. At time 6 min, the extracellular osmolarity was reduced by 33 %, from 300 to 200 mosmol l^{-1}. Efflux rate constants were obtained as described in the legend to Fig. 2. Rates are shown as means + S.E.M. of 6 (wild-type) or 5 (RhoAV14C3) experiments. *B*, dependence of taurine efflux on osmolarity in wild-type and RhoAV14C3 cells. Taurine efflux was measured as above. At time 6 min, the extracellular osmolarity was reduced by the percentage shown. The figure shows the maximal efflux rate constant, obtained at time 6 min after hypotonic exposure, as a function of the decrease in extracellular osmolarity. Rates are shown as means + S.E.M. of 6 (wild-type) or 5 (RhoAV14C3) experiments. Stars indicate that the value in RhoAV14VC3 cells is significantly different from that in wild-type cells. Swelling-activated taurine efflux is significantly different from the isotonic value after a decrease in osmolarity of 20 % or more in the wild-type cells ($P < 0.05$), and 13.3 % or more in RhoAV14C3 cells ($P < 0.05$).

Table 1 shows the effect of Cl^- channel inhibitors on $I_{Cl,swell}$ in wild-type and RhoAV14C3 cells. As seen, the inhibitor profile of $I_{Cl,swell}$ was similar in wild-type and RhoAV14 cells. Niflumic acid (100 μM) and tamoxifen (10 μM) inhibited the current by about 45 % and 80 %, respectively, at both positive and negative potentials. Current inhibition by 4,4′-diisothiocyano-2,2′-stilbene-disulfonic acid (DIDS) (100 μM) was voltage dependent, with about 65 % inhibition at +80 mV, but little and variable effect at −60 mV.

The Cl^- currents elicited in the two strains by a 30 % decrease in bath osmolarity were indistinguishable with respect to activation lag-time, time to half-maximal activation, current magnitude at −60 and +80 mV, and time to half-maximal deactivation upon return to isotonic conditions ($n = 20$ wild-type and 7 for RhoAV14C3, data not shown). To investigate whether the endogenous RhoA activity was sufficient for full activation of the current after the extensive swelling induced by this treatment, we compared the

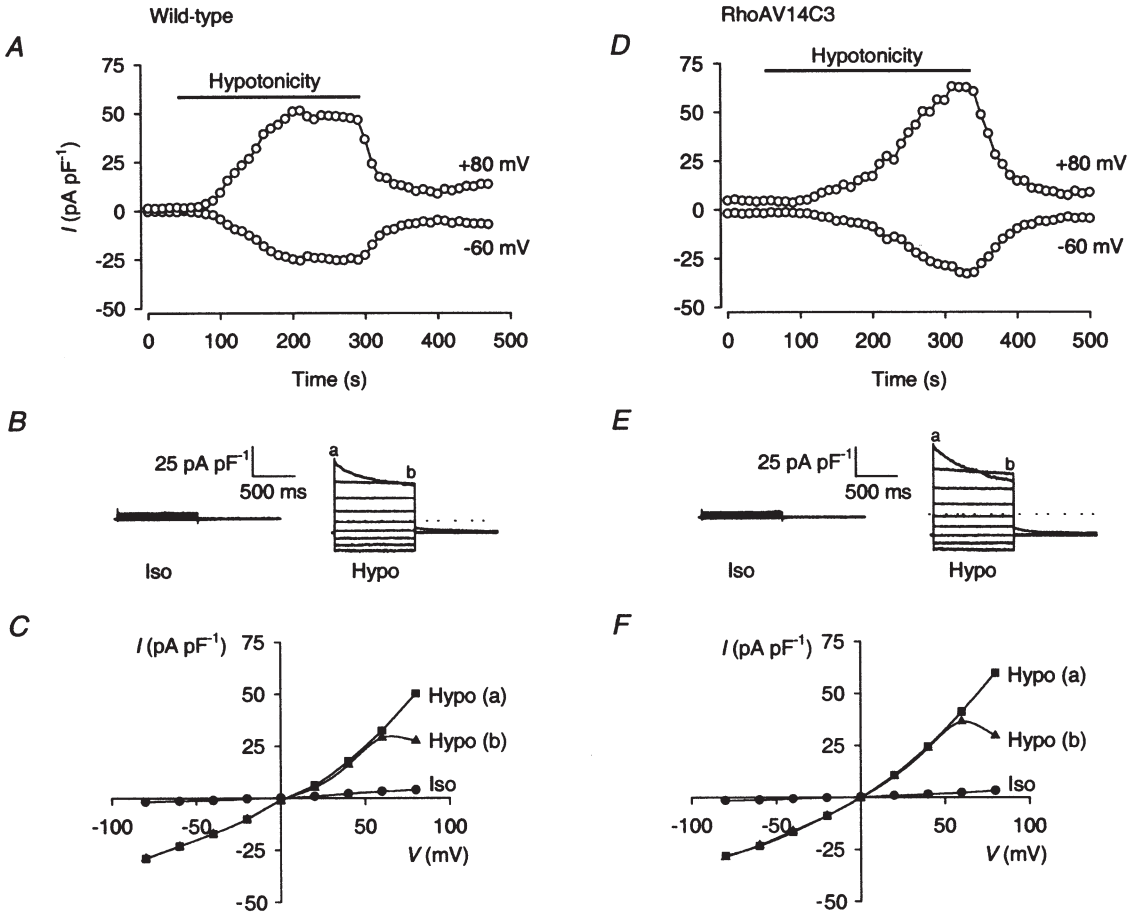

Figure 4. Effect of RhoAV14 expression on $I_{Cl,swell}$

A, time course of the whole-cell membrane currents activated by hypotonic cell swelling in wild-type NIH3T3 cells. Currents were measured using the whole-cell patch-clamp technique, as described in Methods. The isotonic bath solution was replaced by a 30 % hyptonic solution as indicated by the horizontal bar. Current magnitude at +80 and −60 mV normalised to cell size was calculated from data obtained by applying linear ramp protocols (see Methods) every 10 s. The experiment shown is representative of 38 experiments. *B*, voltage-dependent properties of $I_{Cl,swell}$ in wild-type NIH3T3 cells. From the holding potential of −40 mV, 20 mV steps of 1000 ms duration were applied from −80 to +80 mV, under isotonic conditions or 30 % hypotonic conditions as indicated. The traces shown are representative of 6–9 experiments (data in *B* and *C* are from the same cell, data in *A* are from another cell under the same conditions). *C*, current–voltage (*I–V*) relationships calculated from the current traces shown in *B* at *a* and *b*. *D*, time course of the whole-cell membrane currents activated by hypotonic cell swelling in RhoAV14C3 cells. All experimental conditions were as in *A*. The experiment shown is representative of 30 experiments. *E*, voltage-dependent properties of $I_{Cl,swell}$ in RhoAV14C3 NIH3T3 cells. All experimental conditions were as in *B*. The traces shown are representative of 6–9 experiments (data in *E* and *F* are from the same cell, data in *D* are from another cell under the same conditions). *F*, *I–V* relationships calculated from the current traces shown in *E*.

Table 1. Effect of Cl^- channel inhibitors (shown as percentage current inhibition) on $I_{Cl,swell}$ magnitude in wild-type and RhoAV14 NIH3T3 cells

	Tamoxifen (10 μM)			Niflumic acid (100 μM)			DIDS (100 μM)		
	−60 mV	+80 mV	*n*	−60 mV	+80 mV	*n*	−60 mV	+80 mV	*n*
Wild-type	80 ± 10	80 ± 8	3	42 ± 7	46 ± 6	5	n.d.	66 ± 9	5
Rho	77 ± 6	86 ± 3	4	40 ± 2	48 ± 4	5	n.d.	59 ± 14	3

n.d., not determined. Currents were measured using the whole-cell patch-clamp technique, as described in Methods. Linear ramp protocols were applied every 10 s. Tamoxifen (10 μM), DIDS (100 μM), or niflumic acid (100 μM) were applied after full activation of the current by hypotonic exposure (30 %). The percentage inhibition of the current by Cl^- channel inhibitors was calculated from the difference in stable current magnitude before and after perfusion with the inhibitor, after full activation of the current. Data are given as means ± S.E.M. Due to the extremely high variability found for these values, current inhibition by DIDS at −60 mV was not determined (see text for details).

osmosensitivity of $I_{Cl,swell}$ in wild-type and RhoAV14C3 cells. As expected for a swelling-activated current, the relative current increase compared to that measured under isotonic conditions increased as a function of the degree of hypotonic challenge in both wild-type and RhoAV14C3 cells (Fig. 5). After a decrease in bath osmolarity of only 7.5 %, the relative current increase was about twofold higher in RhoAV14-expressing cells than in wild-type cells ($P < 0.02$, $n = 14$ wild-type/15 RhoAV14C3). After decreases in extracellular osmolarity of 15 % and 30 %, there was no significant difference in current magnitude between wild-type and RhoAV14C3 cells.

After a 10 min preincubation with 10 μM Y-27632 , the onset of $I_{Cl,swell}$ was delayed, and the magnitude, measured 3 min after a 30 % decrease in osmolarity, was reduced by about 60 % in wild-type cells, from a current density of 40 ± 8 pA pF^{-1} ($n = 6$) at +80 mV under control conditions to 15 ± 5 pA pF^{-1} after Y-273632 treatment ($n = 5$, $P < 0.05$, Fig. 6). Similarly, $I_{Cl,swell}$ magnitude in wild-type cells after a second hypotonic stimulation was reduced by about 50 % by a 10 min preincubation with 10 μM Y-27632 ($P < 0.05$; $n = 5$ for control and 4 for Y-27632 , data not shown). At 10 μM, Y-27632 does not significantly inhibit p21-activated protein kinase (PAK), PKC, PKA, or MLCK

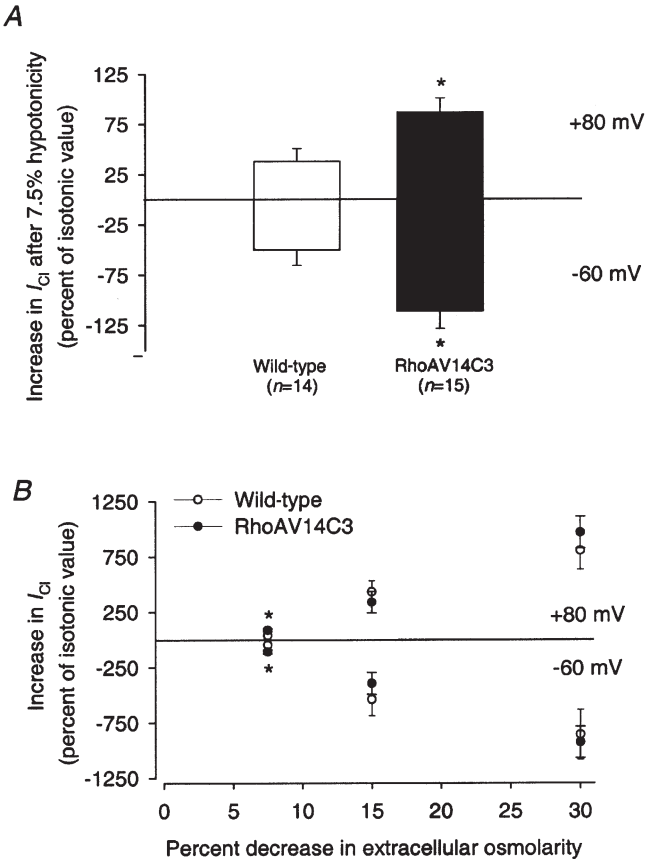

Figure 5. Dependence of $I_{Cl,swell}$ on the magnitude of the hypotonic challenge

A, effect of a 7.5 % decrease in bath osmolarity on the increase in current magnitude in wild-type and RhoAV14C3 cells. Currents were measured using the whole-cell patch-clamp technique, and linear ramp protocols were applied every 10 s. Bath osmolarity was decreased by 7.5 %, and the current was allowed to stabilise. The percentage increases in maximal current magnitude compared to those measured under isotonic conditions were calculated and are shown as means with S.E.M. error bars. * The value in RhoAV14C3 cells is significantly different from that in wild-type cells ($P < 0.05$). *B*, effect of decreases in bath osmolarity on the increase in current magnitude in wild-type and RhoAV14C3 cells. Currents were measured as in *A*, after decreases in bath osmolarity of 7.5 %, 15 %, or 30 %, and were allowed to stabilize. The percentage increase in maximal current magnitude compared to that measured under isotonic conditions was calculated for each osmolarity. Data are shown as means with S.E.M. error bars, the number of experiments was 14–20 for each strain and condition.

(Ishizaki *et al.* 2000). Thus, these findings suggest that a Rho-mediated signal transduction pathway is involved in the regulation of $I_{Cl,swell}$, and that the lack of effect of RhoAV14 expression on $I_{Cl,swell}$ after a 30 % decrease in osmolarity probably reflects that the endogenous RhoA activity under these conditions is sufficient for full activation of $I_{Cl,swell}$ (see also Discussion). In RhoAV14C3 cells, $I_{Cl,swell}$ after a 30 % decrease in osmolarity appeared unaffected by Y-27632 (10 μM, 10 min preincubation) ($P > 0.7$; $n = 4$ for control and 4 for Y-27632, data not shown), suggesting that the high expression of constitutively active RhoA in these cells may not be overcome by Y-27632.

Since the inhibitory effect of Y-27632 on $I_{Cl,swell}$ in CPAE cells has been proposed to involve changes in MLC phosphorylation (Nilius *et al.* 2000), we investigated the effect of the MLCK inhibitor, ML-7, on $I_{Cl,swell}$ after a 30 % decrease in osmolarity (Fig. 7*A* and *B*). As can be seen, in the NIH3T3 cells, ML-7 treatment (10 μM included in the pipette solution) did not inhibit activation of $I_{Cl,swell}$, but on the contrary resulted in a 250 % increase in $I_{Cl,swell}$ magnitude, from a current density at +80 mV of 61 ± 6 pA pF^{-1} ($n = 22$) under control conditions to 150 ± 32 pA pF^{-1} ($n = 6$) with ML-7 in the pipette ($P < 0.0001$). The effect on $I_{Cl,swell}$ was similar when ML-7 was introduced by preincubation (10 μM, 30 min, $n = 1$). Similar to the current in control cells, the ML-7-potentiated $I_{Cl,swell}$ was reversible upon re-exposure to isotonic bath solution ($n = 4$, data not shown).

To further address the possible role of MLCK in the regulation of $I_{Cl,swell}$, we tested the effect of the AV25 peptide, an MLCK inhibitor based on the autoinhibitory domain of MLCK (Weber *et al.* 1999). Inclusion of AV25 (10 μM) in the pipette increased $I_{Cl,swell}$ magnitude after a 30 % decrease in extracellular osmolarity more than 300 %, from 23 ± 11 pA pF^{-1} in control cells dialysed with vehicle only (Tris-HCl pH 7.5, final concentration in the pipette 1 mM) to 79 ± 22 pA pF^{-1} in the presence of AV25 ($n = 7$ for each condition, $P < 0.05$, Fig. 7*C* and *D*). It should be noted that, presumably due to the Tris-HCl vehicle, both control and AV25-treated cells were more fragile than normal and currents, which were measured 4.5 min after hypotonic exposure, were smaller and somewhat delayed compared to the currents measured under the standard hypotonic conditions. Thus, the observation that two unrelated inhibitors of MLCK both potently stimulated $I_{Cl,swell}$ in NIH3T3 cells strongly indicates that MLCK exerts an inhibitory effect on the volume-sensitive Cl^- current.

In many cell types, osmotic cell swelling and shrinkage are associated with a rapid decrease or an increase in cellular F-actin content, respectively (see e.g. Pedersen *et al.* 2001*a*), and we have found this to be the case also in NIH3T3 cells (Pedersen *et al.* 2001*b*). Since both RhoA and MLCK are important modulators of the actin-based cytoskeleton, we tested the possibility that they could be exerting their effects by altering the swelling-induced F-actin changes. After exposure to a 50 % hypotonic solution for 1 min, wild-type cells exhibited a net cellular

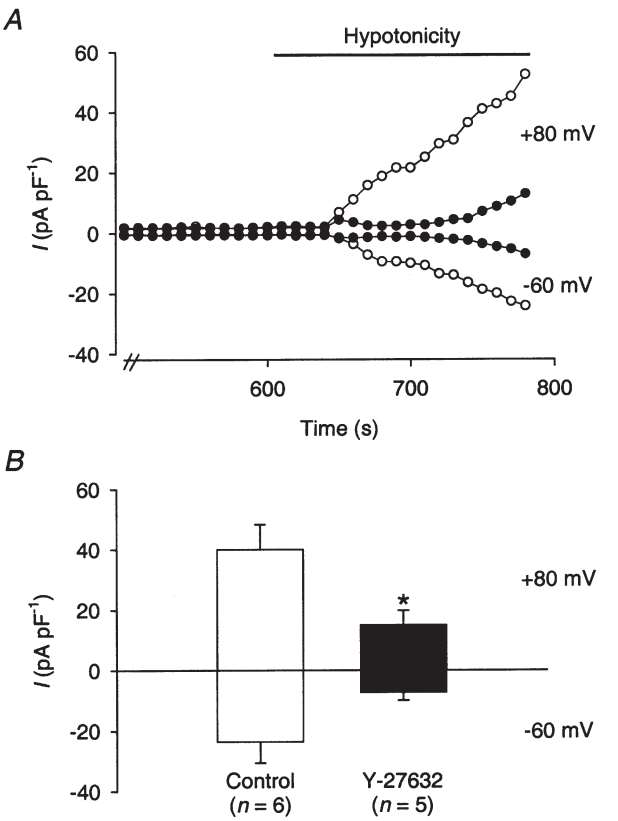

Figure 6. Effect of the ROK/ROCK inhibitor Y-27632 on $I_{Cl,swell}$

A, effect of Y-27632 on the time course of $I_{Cl,swell}$ in wild-type NIH3T3 cells. Cells were pre-incubated with (●) or without (○) Y-27632 (10 μM) for 10 min, prior to exposure to a 30 % hypotonic solution in the continued presence of Y-27632 . Linear voltage ramps were applied every 10 s. The traces shown are representative of 6 (control) and 5 (Y-27632) experiments. It may be noted that current magnitude is about 30 % lower in these control cells than under normal experimental conditions, probably due both to the 10 min period in isotonic solution after obtaining the whole-cell configuration, and to the fact that currents were, in this case, measured 3 min after activation. *B*, effect of Y-27632 on mean current density in wild-type NIH3T3 cells. Experimental conditions as in *A*. Current density was calculated from the current magnitude measured at +80 and −60 mV at time 3 min after hypotonic exposure, divided by cell capacitance. The data are shown as means with S.E.M. error bars. * The value in Y-27632-treated cells is significantly different from that in control cells ($P < 0.05$).

F-actin content of 0.96 ± 0.042 ($n = 7$) relative to that in isotonic control cells as measured using a quantitative rhodamine–phalloidin assay. In RhoAV14-expressing cells, the F-actin content after 1 min of hypotonic exposure was 0.91 ± 0.017 ($n = 3$), not significantly different ($P = 0.46$) from the hypotonic value in wild-type cells. Finally, in wild-type cells preincubated for 30 min with 10 μM ML-7, the F-actin content after 1 min of hypotonic exposure was 0.70 ± 0.113 ($n = 4$), significantly lower than the hypotonic value in wild-type cells ($P < 0.05$).

Possible role of tyrosine kinases in swelling-induced activation of taurine efflux. Tyrosine phosphorylation

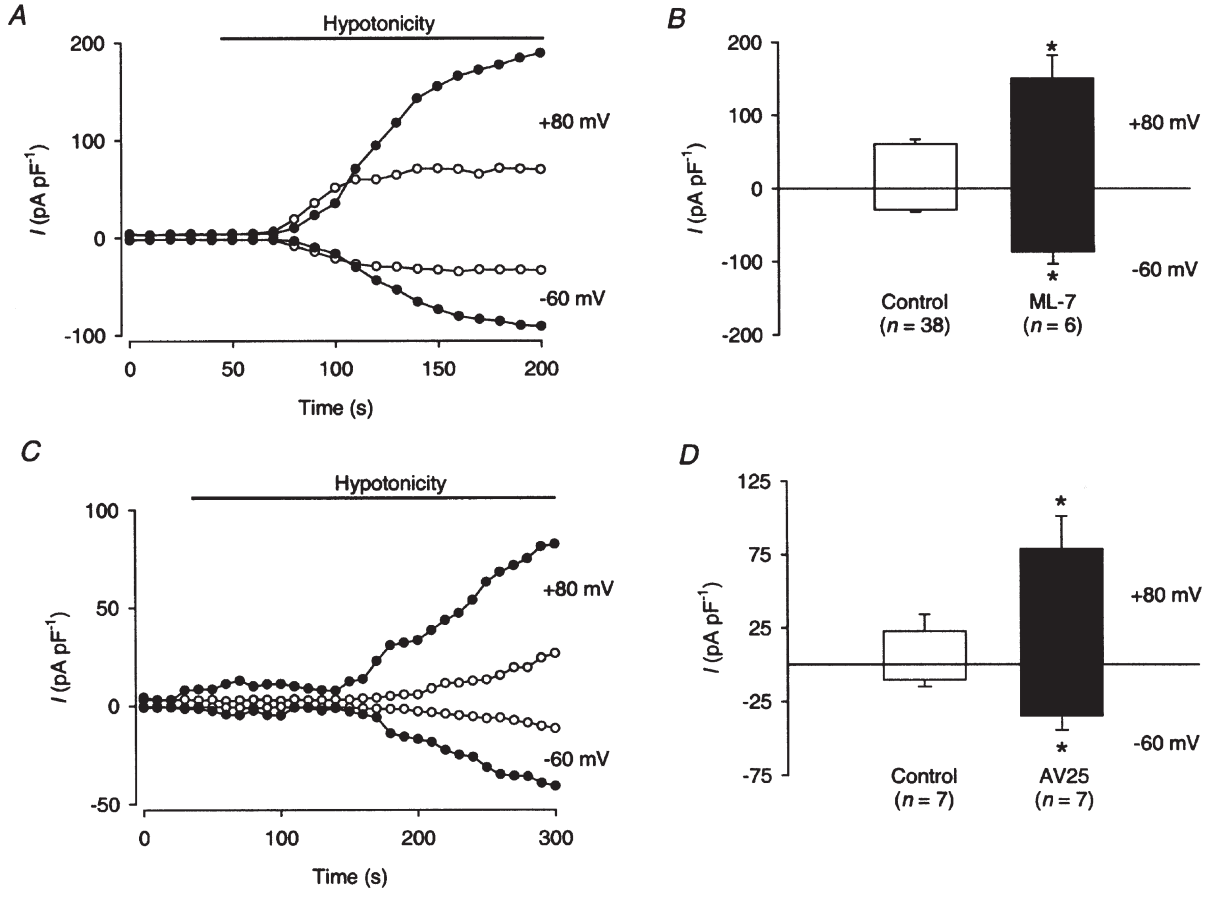

Figure 7. Effect of the MLCK inhibitors ML-7 and AV25 on $I_{Cl,swell}$

A, effect of ML-7 on the time course of $I_{Cl,swell}$ in wild-type NIH3T3 cells. The cells were loaded with ML-7 (10 μM, ●) in the patch pipette for 3 min prior to initiating the experiments. ○, a representative control trace from the same day and passage. Linear voltage ramps were applied every 10 s, and currents measured at +80 and −60 mV. *B*, effect of ML-7 on mean current density in wild-type NIH3T3 cells. Experimental conditions were as described in *A*. Current density was calculated from the current magnitude measured at +80 and −60 mV after full activation of the current by hypotonic exposure, divided by cell capacitance. Data are shown as means with S.E.M. error bars. In two control experiments, it was shown that the inclusion of the ML-7 solvent (ethanol) in the pipette solution at the concentration used in the ML-7 experiments was without effect on $I_{Cl,swell}$, and all other control experiments were therefore performed without inclusion of the solvent. As the current values obtained in the control experiments performed on the same day as the ML-7 experiments were well within the mean ± S.D. of the values obtained in all the control experiments, all control experiments were pooled for the final comparison, and thus the traces shown are representative of 38 (control) and 6 (ML-7) experiments. * The value in ML-7-treated cells is significantly different from that in control cells ($P < 0.0001$). *C*, effect of AV25 on the time course of $I_{Cl,swell}$ in wild-type NIH3T3 cells. The cells were loaded with AV25 (10 μM, ●) in the patch pipette for 3 min prior to initiating the experiments. ○, a representative control trace from the same day and passage, dialysed with vehicle (Tris-HCl, pH 7.5) only. Linear voltage ramps were applied every 10 s, and currents measured at +80 and −60 mV. *D*, effect of AV25 on mean current density in wild-type NIH3T3 cells. Experimental conditions were as described in *A*. Current density was calculated from the current magnitude measured at +80 and −60 mV after 4.5 min of hypotonic exposure (because the vehicle caused the seals to be easily lost upon extensive swelling in both control and AV25-treated cells), divided by cell capacitance. Data are shown as means with S.E.M. error bars. The data shown represent 7 experiments for each condition. * The value in AV25-treated cells is significantly different from that in control cells ($P < 0.05$).

events have been shown to play a role in the RVD process in several cell types, and could, potentially, play a role in the RhoA-mediated stimulation of osmolyte efflux in the NIH3T3 cells (see Introduction). We therefore addressed the possible role of tyrosine phosphorylation events in the swelling-induced activation of taurine efflux in wild-type and RhoAV14-expressing cells, by incubation with the general protein tyrosine phosphatase inhibitor Na_3VO_4 (50 μM) prior to hypotonic exposure. Under isotonic conditions, Na_3VO_4 did not affect the taurine efflux rate in either strain. In contrast, after hypotonic swelling (33 % decrease in extracellular osmolarity) Na_3VO_4 strongly potentiated the taurine efflux in both wild-type and RhoAV14-expressing cells, increasing the maximal rate constant for taurine efflux from 0.031 ± 0.0069 min^{-1} to 0.104 ± 0.0132 min^{-1} in wild-type cells ($n = 3$ paired experiments, $P < 0.04$), and from 0.086 ± 0.0148 min^{-1} to 0.186 ± 0.0091 min^{-1} in RhoAV14C3 cells ($n = 3$ paired experiments, $P < 0.04$). Moreover, the rate constants continued to increase for a longer time after hypotonic exposure in the Na_3VO_4-treated cells, the maximal rate constant being reached approximately 12 min after hypotonic exposure after Na_3VO_4 treatment, compared to about 6 min in control cells.Conversely, after exposure to the general tyrosine kinase inhibitor genistein (100 μM, 6 min preincubation), the swelling-activated taurine efflux was inhibited in both wild-type and RhoAV14-expressing cells, the maximal rate constant for taurine efflux being reduced from 0.029 ± 0.0017 min^{-1} to 0.015 ± 0.0016 min^{-1} in wild-type cells ($n = 3$ paired experiments, $P < 0.01$), and from 0.089 ± 0.0024 min^{-1} to 0.048 ± 0.0023 min^{-1} in RhoAV14C3 cells ($n = 4$ paired experiments, $P < 0.001$). In both strains, the maximal rate constant was reached at time 4 min after hypotonic swelling in genistein-treated cells, compared to time 6 min in control cells. Taken together, these data suggest that tyrosine phosphorylation plays a role in maintaining the open state of the taurine efflux pathway, and that tyrosine dephosphorylation events are involved in the closing of this pathway.

DISCUSSION

Several lines of evidence suggest that GTP binding proteins play an important role in the signalling events activated by cell swelling and eventually resulting in efflux of K^+, Cl^-, and organic osmolytes and restoration of cell volume. The molecular identity of the G protein(s) involved is frequently not clear from the available studies, and both heterotrimeric G proteins and small G proteins of the Rho family have been implicated in the process (see Introduction). The role of Rho in RVD has so far only been studied directly at the level of Cl^- efflux/Cl^- current measurements, and the precise mechanisms remain unelucidated and controversial. Thus, swelling-induced activation of Cl^- efflux was reported to involve (i) Rho-mediated activation of PI3K and FAK in Intestine 407 cells (Tilly *et al.* 1996), (ii) ROK/ROCK and probably MLC phosphorylation in CPAE cells (Nilius *et al.* 1999; Nilius *et al.* 2000), and (iii) phosphorylation-independent events in mouse neuroblastoma cells (Estevez *et al.* 2001). In the present study, we have investigated the possible roles of Rho-mediated signalling events following osmotic cell swelling in NIH3T3 cells, addressing the impact of such events on the RVD process as a whole, as well as on the activity of the individual swelling-activated transporters.

Expression of constitutively active RhoA correlates with acceleration of RVD

Following osmotic cell swelling, wild-type NIH3T3 cells exhibited regulatory volume decrease (RVD), in agreement with previous findings (Pasantes-Morales *et al.* 1997). When a constitutively active RhoA mutant, RhoAV14, was expressed in NIH3T3 cells, the rate of RVD was increased about fourfold. Confirming the relation to RhoA, the extent of RVD acceleration correlated with the level of RhoAV14 expression. Expression of constitutively active Rac1 (Rac1V12) also resulted in an increase in RVD rate, whereas expression of H-Ras did not. Thus, the present findings suggest that activation of RhoA and Rac1, but not H-Ras, can contribute to the activation of osmolyte loss after cell swelling in NIH3T3 cells. The RhoAV14-expressing cells in fact initially shrunk beyond their original isotonic volume. Subsequently, the volume of the RhoAV14C3 cells gradually recovered towards the steady state volume. The initial 'overshoot' did not reflect an impairment of the RVI process, as the rate of RVI following osmotic shrinkage elicited by re-exposure to isotonic medium was in fact slightly higher in the RhoAV14C3 cells compared to wild-type cells; hence, the initial shrinkage below isotonic volume during RVD was apparently too small to trigger RVI. This shrinkage therefore most likely reflects a slightly prolonged opening of the swelling-activated K^+ and Cl^- channels. Thus, as long as the membrane potential remains between the equilibrium potentials for Cl^- and K^+ and both channel types remain open, the cells will continue to shrink, regardless of their original volume set point.

The RhoAV14-induced increase in RVD rate could not be explained by changes in the effect of hypotonic exposure on $[Ca^{2+}]_i$ or on the extent of osmotic cell swelling. Moreover, in wild-type cells the RVD rate was essentially unaffected by treatment with Y-27632 or wortmannin, arguing against a role for either ROK/ROCK or PI3K in the process. It should also be noted that although increased surface area *per se* might be associated with an increased number of transporters per cell, the 30 % larger cell surface area in the RhoAV14C3 cells is far from sufficient to account for the several-fold increases in RVD, K^+ and taurine efflux rates in these cells compared to wild-type cells. Further supporting the notion that the transport

rates do not simply correlate with surface area, the raw $I_{Cl,swell}$ current (i.e. not normalised to cell capacitance) elicited by 30 % hypotonic challenges is not increased in the RhoAV14C3 cells. The reason for this is not known, but one possibility is that the density of these transporters in the plasma membrane is slightly decreased in the RhoAV14-expressing strain.

RhoA and Rac1, which had comparable effects on RVD, also share several effectors (e.g. PI4, 5K, PI3K, DAG kinase, and PLD kinase) which affect the actin cytoskeleton (Bishop & Hall, 2000; Takai *et al.* 2001). As in most other cell types, RVD in NIH3T3 cells involves the activation of efflux pathways for K^+, Cl^-, and organic osmolytes such as taurine (Pasantes-Morales *et al.* 1997). Therefore, we investigated in turn the possible role of Rho in the regulation of each of these efflux pathways.

Swelling-activated K^+ efflux: identity and stimulation by RhoAV14

The swelling-activated K^+ efflux from NIH3T3 cells after a 33 % decrease in osmolarity was about doubled in the strain with maximal RhoAV14 expression compared to that measured in wild-type cells, and the volume set point appeared lowered in the absence of effects on the time course of activation. RVD in NIH3T3 cells has previously been found to be accelerated by the K^+ ionophore gramicidin, suggesting that K^+ efflux is the rate-limiting factor (Pasantes-Morales *et al.* 1997). In agreement with this, we found that the increased rate of K^+ efflux induced by RhoAV14 expression could significantly enhance the RVD rate after severe osmotic challenges, in spite of a lack of effect of RhoA on the current carried by the counterion, Cl^-, under these conditions. In further support of the notion that K^+ efflux is rate limiting for the RVD, inhibition of ROK/ROCK in wild-type cells, which strongly reduced $I_{Cl,swell}$ but did not affect the swelling-activated K^+ or taurine efflux, also did not inhibit RVD. Previous studies have suggested the activation of separate anion and K^+ efflux pathways by osmotic swelling in NIH3T3 cells (Pasantes-Morales *et al.* 1997), but the molecular identity of the latter is unknown. The present findings that this pathway is partially inhibited by furosemide, Ba^{2+} and TEA, but unaffected by a broad spectrum of other K^+ channel inhibitors, suggest that the K^+ efflux activated by cell swelling in NIH3T3 cells is mediated in part by K^+–Cl^- cotransport, and in part by as yet unidentified K^+ channel(s).

Swelling-activated taurine efflux: identity and stimulation by RhoAV14

Net loss of the organic osmolyte taurine contributes significantly to the RVD process in most mammalian cell types including NIH3T3 cells (Moran *et al.* 1997). RhoAV14 expression resulted in approximate doubling of the rate constant for taurine efflux at all osmolarities tested, apparently associated with a slight lowering of the volume set point. Although the swelling-activated taurine efflux in NIH3T3 cells has previously been studied, it is unknown whether swelling-activated taurine and Cl^- efflux is mediated by the same or different pathways in these cells (Moran *et al.* 1997). The present finding that the swelling-activated efflux of these osmolytes is differentially regulated by Rho may suggest the existence of separate taurine and Cl^- efflux pathways in these cells.

RhoA modulates the volume sensitivity of $I_{Cl,swell}$

Following swelling in hypotonic medium, a Ca^{2+}-independent Cl^- current exhibiting moderate outward rectification and time-dependent inactivation at depolarised potentials was activated in both RhoAV14-expressing and wild-type NIH3T3 cells. The current characteristics were typical of the swelling-activated Cl^- current in many cell types (see Okada, 1997), and in good agreement with some studies on $I_{Cl,swell}$ in NIH3T3 cells (e.g. Luckie *et al.* 1994; Gschwentner *et al.* 1995). It may, however, be noted that other authors have been unable to demonstrate the presence of endogenous swelling-activated Cl^- currents in NIH3T3 cells (Gill *et al.* 1992; Valverde *et al.* 1992), possibly reflecting differences between the many strains of NIH3T3 cells.

The Cl^- current activated after a 30 % decrease in bath osmolarity was similar with respect to all characteristics studied in wild-type and RhoAV14C3 cells. However, this seems to reflect that the current is already maximally activated under these conditions, since after a more physiologically relevant hypotonic challenge (7.5 % decrease in osmolarity), the increase in $I_{Cl,swell}$ magnitude was approximately doubled in RhoAV14C3 cells compared to wild-type cells. This suggests that RhoA may be involved in modulation of the volume set point of $I_{Cl,swell}$, in apparent agreement with previous findings in bovine endothelial cells (Voets *et al.* 1998). In contrast, in mouse neuroblastoma cells, the $I_{Cl,swell}$ volume set point was increased by GDPβS, but unaffected by inhibition of Rho, Rac and Cdc42 by *Clostridium difficile* toxin B (Estevez *et al.* 2001).

Inhibition of ROK/ROCK by Y-27632 significantly reduced the magnitude of $I_{Cl,swell}$ in wild-type NIH3T3 cells. Preliminary Western blot analyses ($n = 2$) using an antibody against ROK/ROCK indicate that one or both ROK/ROCK isoforms are present in the 3T3 cells, although several unspecific bands of lower molecular weight were also detected. Multiple targets and effects downstream of ROK/ROCK have been identified or proposed (see below). One of these is increased MLC phosphorylation, an effect which is thought to be mainly mediated *in vivo* by ROK/ROCK-mediated inhibition of myosin phosphatase, and therefore to be at least in part dependent on the activity of MLCK (Somlyo & Somlyo, 2000). Indeed, $I_{Cl,swell}$ in CPAE cells was inhibited by the MLCK inhibitor ML-9 and by MLCK inhibitor peptides

(Nilius *et al.* 2000). Interestingly, in the present study, inclusion of either the MLCK inhibitor ML-7, or the MLCK inhibitory peptide AV25 in the pipette had no inhibitory effect on $I_{Cl,swell}$, but on the contrary dramatically increased current magnitude in wild-type cells, strongly suggesting that MLCK exerts an inhibitory effect on $I_{Cl,swell}$ in these cells. Our data appear to be in congruence with findings suggesting that MLCK, conversely, plays an important role in the activation of several transporters involved in the regulatory volume increase (RVI) after osmotic cell shrinkage (Krarup *et al.* 1998; Shrode *et al.* 1995; see e.g. Hoffmann & Pedersen, 1998). Several possible mechanisms for the stimulating effect of MLCK inhibition on $I_{Cl,swell}$ may be proposed. Since MLCK has been found to play an important role in resistance to osmotic stress (Cai *et al.* 1998), it is conceivable that MLCK inhibition could augment osmotic swelling and/or membrane unfolding, both of which are expected to increase $I_{Cl,swell}$ (Okada, 1997). This notion is supported by the present finding that inhibition of MLCK strongly potentiates swelling-induced F-actin depolymerisation, an effect presumably reflecting a weakening of the cortical F-actin-myosin II network (see e.g. Bresnick, 1999). In contrast, RhoAV14 overexpression was not associated with a significant change in the swelling-induced F-actin depolymerisation. Given the lack of effect of RhoA on $I_{Cl,swell}$ after decreases in osmolarity of more than 7.5 %, this is not incompatible with a role of the actin-based cytoskeleton in the effect of RhoA. However, further experiments are needed to directly address this, and the detection level of our current methods does not allow evaluation of differences in F-actin changes after very mild osmotic swelling. Interestingly, the stimulation of $I_{Cl,swell}$ by RhoA may actually involve the previously described feedback inhibition of MLCK by Rho family G proteins (Somlyo & Somlyo, 2000). While the most well described effect of ROK/ROCK activation is increased MLC phosphorylation, the divergent effects of ROK/ROCK and MLCK on $I_{Cl,swell}$ suggested by the present findings are not surprising. Thus, firstly, the relative roles of MLCK and ROK/ROCK in MLC phosphorylation *in vivo* are far from interchangeable, but differ with e.g. subcellular location (e.g. Totsukawa *et al.* 2000). Secondly, many ROK/ROCK substrates other than MLC and myosin phosphatase have been described; those of potential relevance for volume sensing and signalling include the actin regulatory proteins calponin and adducin, intermediate filament proteins, and moesin of the ezrin/radixin/moesin (ERM) family of proteins involved in membrane-cytoskeleton interaction (Kaneko *et al.* 2000; see Amano *et al.* 2000). Future studies are needed to establish the mechanism involved in the inhibitory effect of MLCK, and the potential role of such other effectors in the regulation of $I_{Cl,swell}$, or indeed in the volume-sensing pathway of NIH3T3 cells.

Role of protein tyrosine kinases in RVD

The swelling-activated efflux of taurine was strongly potentiated by the protein tyrosine phosphatase inhibitor Na_3VO_4, and inhibited by the general tyrosine kinase inhibitor genistein, in both wild-type and RhoAV14C3 cells, in agreement with previous data suggesting a role for tyrosine kinases in the regulation of swelling-activated taurine efflux in other cells (Deleuze *et al.* 2000; Lambert & Falktoft, 2000). This appeared to reflect that the taurine efflux pathway open time was prolonged by Na_3VO_4 and reduced by genistein, as judged by the time from hypotonic swelling to the point at which the maximal efflux rate constant was reached. Although further investigations should be conducted to unequivocally determine the possible relationship between RhoA- and tyrosine phosphorylation-mediated stimulation of taurine efflux, two of the present findings strongly suggest that the two are at least partially independent events: (i) in contrast to the effects of tyrosine phosphorylation/dephosphorylation, the stimulation elicited by RhoAV14 expression does not involve a change in the time taken to reach the maximal efflux rate constant; and (ii) in wild-type cells, the maximal rate constant is reduced by 50 % by genistein, and approximately tripled by Na_3VO_4 treatment, while in RhoAV14-expressing cells, the maximal rate constant is only reduced by about 33 % by genistein, and approximately doubled by Na_3VO_4 treatment. Taken together, this seems to indicate the presence in the RhoAV14-expressing cells of an additional mechanism not affected by tyrosine kinase inhibition.

Possible upstream role of RhoA in RVD and mechanisms of activation of Rho by cell swelling

The integrated approach applied in the present study, using combined measurements of cell volume, Cl^-, K^+ and taurine efflux, revealed for the first time that RhoA plays multiple roles in the RVD process. Thus, introduction of constitutively active RhoA potently stimulates the net RVD process, and the findings strongly indicate that it does so by stimulating the same efflux pathways as those involved in RVD in wild-type cells. In the wild-type NIH3T3 cells, ROK/ROCK plays a major role in the signalling pathway from RhoA to $I_{Cl,swell}$, while the modulation by RhoA of the volume-activated K^+ and taurine channels occurs via a different signalling pathway. RhoA thus seems to be an upstream modulator shared by the swelling-activated osmolyte transporters, yet acting on these transporters via divergent signalling pathways. While further studies are needed to delineate the precise pathways of the RhoA-mediated modulation of the individual transporters, this suggests an important role of RhoA in the overall control of the RVD process. We have at present no evidence to distinguish between a permissive role of RhoA or a direct activation of RhoA by cell swelling, and it is possible, as suggested by a recent study in vascular

endothelial cells (Carton *et al.* 2002), that the role of RhoA is a permissive one. If RhoA is indeed activated by cell swelling, this could be initiated by mechanically induced changes in signalling via integrins and/or receptors coupled to heterotrimeric G proteins, such as various growth factor receptors, many of which are known to activate Rho family G proteins (see e.g. Sah *et al.* 2000). As both RhoA and Rac1 have been shown to preferentially localise to caveolae (Michaely *et al.* 1999), swelling-induced Rho activation could also be initiated via changes in caveolae organisation evoked by the swelling-induced membrane unfolding and/or cytoskeletal reorganisation. Indeed, caveolin-1, which appears to interact directly with RhoA (Gingras *et al.* 1998), has been suggested to modulate $I_{Cl,swell}$ activity in endothelial cells (Trouet *et al.* 1999; Trouet *et al.* 2001). It should be kept in mind, however, that while RhoA activation clearly stimulates the swelling-activated efflux of Cl^-, taurine and K^+, the present study also demonstrates that RhoA activation is not sufficient to explain volume sensing *per se*, since constitutive RhoA activity does not lead to activation of the swelling-activated efflux pathways under isotonic conditions.

In conclusion, expression of constitutively active RhoA increases the rate of RVD in NIH3T3 cells, in a Ca^{2+}-independent manner. After substantial hypotonic challenge, this mainly reflects a stimulation of K^+ and taurine efflux by RhoA. For $I_{Cl,swell}$, modulation of the volume set point by RhoA seems to play an important role in current activation after a more physiologically relevant hypotonic challenge. The RVD process, as well as the swelling-activated K^+ and taurine efflux is unaffected by inhibition of ROK/ROCK. In contrast, inhibition of ROK/ROCK inhibits, and inhibition of MLCK strongly potentiates, $I_{Cl,swell}$ and stimulates the disintegration of F-actin after cell swelling. Inhibition of tyrosine phosphatases stimulates, and inhibition of tyrosine kinases inhibits, swelling-activated taurine efflux, apparently via a mechanism that is at least partly different from that involved in RhoA-mediated efflux stimulation. It is suggested that RhoA, although not the volume sensor *per se*, is an important upstream modulator shared by multiple swelling-activated channels on which RhoA exerts its effects via divergent signalling pathways.

REFERENCES

Amano, M., Fukata, Y. & Kaibuchi, K. (2000). Regulation and functions of Rho-associated kinase. *Experimental Cell Research* **261**, 44–51.

Aznar, S. & Lacal, J. C. (2001). Rho signals to cell growth and apoptosis. *Cancer Letters* **165**, 1–10.

Bishop, A. & Hall, A. (2000). Rho GTPases and their effector proteins. *Biochemical Journal* **348**, 241–255.

Bresnick, A. R. (1999). Molecular mechanisms of nonmuscle myosin-II regulation. *Current Opinion in Cell Biology* **11**, 26–33.

Cai, S., Pestic-Dragovich, L., O'Donnell, M. E., Wang, N., Ingber, D., Elson, E. & De Lanerolle, P. (1998). Regulation of cytoskeletal mechanics and cell growth by myosin light chain phosphorylation. *American Journal of Physiology* **275**, C1349–1356.

Cantiello, H. F., Prat, A. G., Bonventre, J. V., Cunningham, C. C., Hartwig, J. H. & Ausiello, D. A. (1993). Actin-binding protein contributes to cell volume regulatory ion channel activation in melanoma cells. *Journal of Biological Chemistry* **268**, 4596–4599.

Carton, I., Trouet, D., Hermans, D., Barth, H., Aktories, K., Droogmans, G., Jorgensen, N.K., Hoffmann, E.K., Nilius, B. & Eggermont, J. (2002).The Rho pathway exerts a permissive effect on volume-regulated anion channels in vascular endothelial cells. *American Journal of Physiology* (in the Press)

Deleuze, C., Duvoid, A., Moos, F. C. & Hussy, N. (2000). Tyrosine phosphorylation modulates the osmosensitivity of volume-dependent taurine efflux from glial cells in the rat supraoptic nucleus. *Journal of Physiology* **523**, 291–299.

Ding, M., Eliasson, C., Betsholtz, C., Hamberger, A. & Pekny, M. (1998). Altered taurine release following hypotonic stress in astrocytes from mice deficient for GFAP and vimentin. *Brain Research. Molecular Brain Research* **62**, 77–81.

Estevez, A. Y., Bond, T. & Strange, K. (2001). Regulation of $I_{Cl,swell}$ in neuroblastoma cells by G protein signaling pathways. *American Journal of Physiology* **281**, C89–98.

Gill, D. R., Hyde, S. C., Higgins, C. F., Valverde, M. A., Mintenig, G. M. & Sepúlveda, F. V. (1992). Separation of drug transport and chloride channel functions of the human multidrug resistance P-glycoprotein. *Cell* **71**, 23–32.

Gingras, D., Gauthier, F., Lamy, S., Desrosiers, R. R. & Beliveau, R. (1998). Localization of RhoA GTPase to endothelial caveolae-enriched membrane domains. *Biochemical and Biophysical Research Communications* **247**, 888–893.

Gschwentner, M., Nagl, U. O., Woll, E., Schmarda, A., Ritter, M. & Paulmichl, M. (1995). Antisense oligonucleotides suppress cell-volume-induced activation of chloride channels. *Pflügers Archiv* **430**, 464–470.

Gudi, S., Nolan, J. P. & Frangos, J. A. (1998). Modulation of GTPase activity of G proteins by fluid shear stress and phospholipid composition. *Proceedings of the National Academy of Sciences of the USA* **95**, 2515–2519.

Hallows, K. R., Packman, C. H. & Knauf, P. A. (1991). Acute cell volume changes in anisotonic media affect F-actin content of HL-60 cells. *American Journal of Physiology* **261**, C1154–1161.

Henson, J. H. (1999). Relationships between the actin cytoskeleton and cell volume regulation. *Microscopy Research and Technique* **47**, 155–162.

Hoffmann, E. K. & Dunham, P. B. (1995). Membrane mechanisms and intracellular signalling in cell volume regulation. *International Review of Cytology* **161**, 173–262.

Hoffmann, E. K. & Hougaard, C. (2001). Intracellular signalling involved in activation of the volume-sensitive K^+ current in Ehrlich ascites tumour cells. *Comparative Biochemistry and Physiology* **130**, 355–366.

Hoffmann, E. K. & Mills, J. W. (1999). Membrane events involved in volume regulation. In *Current Topics in Membranes,* pp. 123–195. Academic Press, San Diego, CA, USA.

Hoffmann, E. K. & Pedersen, S. F. (1998). Sensors and signal transduction in the activation of cell volume regulatory ion transport systems. *Contributions to Nephrology* **123**, 50–78.

Ishizaki, T., Uehata, M., Tamechika, I., Keel, J., Nonomura, K., Maekawa, M. & Narumiya, S. (2000). Pharmacological properties of Y-27632 , a specific inhibitor of rho-associated kinases. *Molecular Pharmacology* **57**, 976–983.

KANEKO, T., AMANO, M., MAEDA, A., GOTO, H., TAKAHASHI, K., ITO, M. & KAIBUCHI, K. (2000). Identification of calponin as a novel substrate of Rho-kinase. *Biochemical and Biophysical Research Communications* **273**, 110–116.

KOYAMA, T., OIKE, M. & ITO, Y. (2001). Involvement of Rho-kinase and tyrosine kinase in hypotonic stress- induced ATP release in bovine aortic endothelial cells. *Journal of Physiology* **532**, 759–769.

KRARUP, T., JAKOBSEN, L. D., JENSEN, B. S. & HOFFMANN, E. K. (1998). Na^+–K^+–$2Cl^-$ cotransport in Ehrlich cells: regulation by protein phosphatases and kinases. *American Journal of Physiology* **275**, C239–250.

LAMBERT, I. H. (1989). Leukotriene-D4 induced cell shrinkage in Ehrlich ascites tumor cells. *Journal of Membrane Biology* **108**, 165–176.

LAMBERT, I. H. & FALKTOFT, B. (2000). Lysophosphatidylcholine induces taurine release from HeLa cells. *Journal of Membrane Biology* **176**, 175–185.

LANG, F., BUSCH, G. L., RITTER, M., VOLKL, H., WALDEGGER, S., GULBINS, E. & HÄUSSINGER, D. (1998). Functional significance of cell volume regulatory mechanisms. *Physiological Reviews* **78**, 247–306.

LUCKIE, D. B., KROUSE, M. E., HARPER, K. L., LAW, T. C. & WINE, J. J. (1994). Selection for MDR1/P-glycoprotein enhances swelling-activated K^+ and Cl^- currents in NIH/3T3 cells. *American Journal of Physiology* **267**, C650–658.

MARGALIT, A., LIVNE, A. A., FUNDER, J. & GRANOT, Y. (1993). Initiation of RVD response in human platelets: mechanical-biochemical transduction involves pertussis-toxin-sensitive G protein and phospholipase A2. *Journal of Membrane Biology* **136**, 303–311.

MCMANUS, M., FISCHBARG, J., SUN, A., HEBERT, S. & STRANGE, K. (1993). Laser light-scattering system for studying cell volume regulation and membrane transport processes. *American Journal of Physiology* **265**, C562–570.

MICHAELY, P. A., MINEO, C., YING, Y. S. & ANDERSON, R. G. (1999). Polarized distribution of endogenous Rac1 and RhoA at the cell surface. *Journal of Biological Chemistry* **274**, 21430–21436.

MORAN, J., MIRANDA, D., PENA-SEGURA, C. & PASANTES-MORALES, H. (1997). Volume regulation in NIH/3T3 cells not expressing P-glycoprotein. II. Chloride and amino acid fluxes. *American Journal of Physiology* **272**, C1804–1809.

NILIUS, B., PRENEN, J., WALSH, M. P., CARTON, I., BOLLEN, M., DROOGMANS, G. & EGGERMONT, J. (2000). Myosin light chain phosphorylation-dependent modulation of volume-regulated anion channels in macrovascular endothelium. *FEBS Letters* **466**, 346–350.

NILIUS, B., VOETS, T., PRENEN, J., BARTH, H., AKTORIES, K., KAIBUCHI, K., DROOGMANS, G. & EGGERMONT, J. (1999). Role of Rho and Rho kinase in the activation of volume-regulated anion channels in bovine endothelial cells. *Journal of Physiology* **516**, 67–74.

OKADA, Y. (1997). Volume expansion-sensing outward-rectifier Cl^- channel: fresh start to the molecular identity and volume sensor. *American Journal of Physiology* **273**, C755–789.

PASANTES-MORALES, H., SANCHEZ, O. R., MIRANDA, D. & MORAN, J. (1997). Volume regulation in NIH/3T3 cells not expressing P-glycoprotein. I. Regulatory volume decrease. *American Journal of Physiology* **272**, C1798–1803.

PEDERSEN, S. F., HOFFMANN, E. K. & MILLS, J. W. (2001*a*). The cytoskeleton and cell volume regulation. *Comparative Biochemistry and Physiology* **130**, 385–399.

PEDERSEN, S. F., MILLS, J. W. & HOFFMANN, E. K. (1999). Role of the F-actin cytoskeleton in the RVD and RVI processes in Ehrlich ascites tumor cells. *Experimental Cell Research* **252**, 63–74.

PEDERSEN, S. F., PEDERSEN, S., JENSEN, K. H. & HOFFMANN, E. K. (2001*b*). Osmotically induced F-actin alterations in NIH 3T3 cells: effects of Rho GTPases and protein kinases, and possible role in cell volume regulation. *Pflügers Archiv* **441**, P21–13.

RIDLEY, A. J. & HALL, A. (1992). The small GTP-binding protein rho regulates the assembly of focal adhesions and actin stress fibers in response to growth factors. *Cell* **70**, 389–399.

RIDLEY, A. J., PATERSON, H. F., JOHNSTON, C. L., DIEKMANN, D. & HALL, A. (1992). The small GTP-binding protein rac regulates growth factor-induced membrane ruffling. *Cell* **70**, 401–410.

SAH, V. P., SEASHOLTZ, T. M., SAGI, S. A. & BROWN, J. H. (2000). The role of Rho in G protein-coupled receptor signal transduction. *Annual Review of Pharmacology and Toxicology* **40**, 459–489.

SCHWARTZ, M. A. & SHATTIL, S. J. (2000). Signaling networks linking integrins and rho family GTPases. *Trends in Biochemical Sciences* **25**, 388–391.

SHEN, M. R., CHOU, C. Y., WU, M. L. & HUANG, K. E. (1998). Differential osmosensing signalling pathways and G-protein involvement in human cervical cells with different tumour potential. *Cellular Signalling* **10**, 113–120.

SHIMIZU, T., MORISHIMA, S. & OKADA, Y. (2000). Ca^{2+}-sensing receptor-mediated regulation of volume-sensitive Cl^- channels in human epithelial cells. *Journal of Physiology* **528**, 457–472.

SHRODE, L. D., KLEIN, J. D., O'NEILL, W. C. & PUTNAM, R. W. (1995). Shrinkage-induced activation of Na^+/H^+ exchange in primary rat astrocytes: role of myosin light-chain kinase. *American Journal of Physiology* **269**, C257–266.

SOMLYO, A. P. & SOMLYO, A. V. (2000). Signal transduction by G-proteins, rho-kinase and protein phosphatase to smooth muscle and non-muscle myosin II. *Journal of Physiology* **522**, 177–185.

TAKAI, Y., SASAKI, T. & MATOZAKI, T. (2001). Small GTP-binding proteins. *Physiological Reviews* **81**, 153–208.

THOROED, S. M., LAURITZEN, L., LAMBERT, I. H., HANSEN, H. S. & HOFFMANN, E. K. (1997). Cell swelling activates phospholipase A2 in Ehrlich ascites tumor cells. *Journal of Membrane Biology* **160**, 47–58.

TILLY, B. C., EDIXHOVEN, M. J., TERTOOLEN, L. G., MORII, N., SAITOH, Y., NARUMIYA, S. & DE JORGE, H. R. (1996). Activation of the osmo-sensitive chloride conductance involves P21rho and is accompanied by a transient reorganization of the F-actin cytoskeleton. *Molecular Biology of the Cell* **7**, 1419–1427.

TOTSUKAWA, G., YAMAKITA, Y., YAMASHIRO, S., HARTSHORNE, D. J., SASAKI, Y. & MATSUMURA, F. (2000). Distinct roles of ROCK (Rho-kinase) and MLCK in spatial regulation of MLC phosphorylation for assembly of stress fibers and focal adhesions in 3T3 fibroblasts. *Journal of Cell Biology* **150**, 797–806.

TROUET, D., HERMANS, D., DROOGMANS, G., NILIUS, B. & EGGERMONT, J. (2001). Inhibition of volume-regulated anion channels by dominant-negative caveolin-1. *Biochemical and Biophysical Research Communications* **284**, 461–465.

TROUET, D., NILIUS, B., JACOBS, A., REMACLE, C., DROOGMANS, G. & EGGERMONT, J. (1999). Caveolin-1 modulates the activity of the volume-regulated chloride channel. *Journal of Physiology* **520**, 113–119.

UEHATA, M., ISHIZAKI, T., SATOH, H., ONO, T., KAWAHARA, T., MORISHITA, T., TAMAKAWA, H., YAMAGAMI, K., INUI, J., MAEKAWA, M. & NARUMIYA, S. (1997). Calcium sensitization of smooth muscle mediated by a Rho-associated protein kinase in hypertension. *Nature* **389**, 990–994.

VALVERDE, M. A., DIAZ, M., SEPÚLVEDA, F. V., GILL, D. R., HYDE, S. C. & HIGGINS, C. F. (1992). Volume-regulated chloride channels associated with the human multidrug-resistance P-glycoprotein. *Nature* **355**, 830–833.

Voets, T., Manolopoulos, V., Eggermont, J., Ellory, C., Droogmans, G. & Nilius, B. (1998). Regulation of a swelling-activated chloride current in bovine endothelium by protein tyrosine phosphorylation and G proteins. *Journal of Physiology* **506**, 341–352.

Weber, L. P., Van Lierop, J. E. & Walsh, M. P. (1999). Ca^{2+}-independent phosphorylation of myosin in rat caudal artery and chicken gizzard myofilaments. *Journal of Physiology* **516**, 805–824.

Willumsen, B. M. (1995). Analysis of ras acylation sites: mutagenesis and transfection. *Methods in Enzymology* **250**, 269–284.

Willumsen, B. M., Vass, W. C., Velu, T. J., Papageorge, A. G., Schiller, J. T. & Lowy, D. R. (1991). The bovine papillomavirus E5 oncogene can cooperate with ras: identification of p21 amino acids critical for transformation by c-rasH but not v-rasH. *Molecular and Cellular Biology* **11**, 6026–6033.

Acknowledgements

The authors wish to express their gratitude to Welfide Corporation, Osaka, Japan, for the kind gift of Y-27632 , and Professor M. P. Walsh, University of Calgary, Canada, for the kind gift of AV25. This work was supported by the Danish National Research Council (9801946 and 9601404), the Carlsberg foundation (970438/40-1256 and 990209/20-840), 'Fonden af 1870' (10.269, I.H.L.), 'The Leo and Karen M. Nielsen's grant for basic medical research' (LN 07/00, I.H.L.), and Novo Nordic (K.H.B.). Dorthe Nielsen and Birthe J. Hansen are gratefully acknowledged for expert technical assistance, and Dr N. K. Jørgensen, Panum Institute, Copenhagen, for help with the establishment of combined light scatter/fluorescence measurements.